

U.S. DEPARTMENT OF COMMERCE
National Technical Information Service

AD-A034 198

MACHINE CASTING OF FERROUS ALLOYS

ABEX CORPORATION, MAHWAH, N.J.

AUGUST 1976

012004

ADA034198



AD

AMMRC CTR 76-25

MACHINE CASTING OF FERROUS ALLOYS

August 1976

H. R. LARSON, B. A. HEYER and C. P. BISWAS

Abex Corporation

Research Center

Mahwah, N. J. 07430

Final Report

Contract Number DAAG46-73-C-0113

Sponsored by: Defense Advanced Research Projects Agency, ARPA Order No. 2267

Program Code No. 4D10

Effective Date of Contract: February 1, 1973

Contract Expiration Date: June 30, 1975

Amount of Contract: \$239,358.00

Contract Period Covered by Report: 1 February 1973-30 September 1975

The views and conclusions contained in this document are those of the authors and should not be interpreted as necessarily representing the official policies, either expressed or implied, of the Defense Advanced Research Projects Agency of the U.S. Government.

Approved for public release; distribution unlimited.

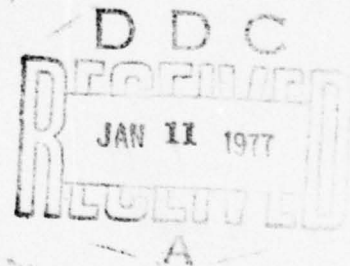
Prepared for

ARMY MATERIALS AND MECHANICS RESEARCH CENTER

Watertown, Massachusetts 02172

REPRODUCED BY
NATIONAL TECHNICAL
INFORMATION SERVICE
U. S. DEPARTMENT OF COMMERCE
SPRINGFIELD, VA. 22161

ORIGINAL CONTAINS COLOR PLATES: ALL DDC
REPRODUCTIONS WILL BE IN BLACK AND WHITE



The view and conclusions contained in this document are those of the authors and should not be interpreted as necessarily representing the official policies, either expressed or implied, of the Advanced Research Projects Agency or the U. S. Government.

The findings in this report are not to be construed as an official Department of the Army position, unless so designated by other authorized documents.

Mention of any trade names or manufacturers in this report shall not be construed as advertising nor as an official indorsement or approval of such products or companies by the United States Government.

DISPOSITION INSTRUCTIONS

Destroy this report when it is no longer needed.
Do not return it to the originator.

UNCLASSIFIED

SECURITY CLASSIFICATION OF THIS PAGE (When Data Entered)

REPORT DOCUMENTATION PAGE		READ INSTRUCTIONS BEFORE COMPLETING FORM
1. REPORT NUMBER AMMRC CTR 76-25	2. GOVT ACCESSION NO.	3. RECIPIENT'S CATALOG NUMBER
4. TITLE (and Subtitle) MACHINE CASTING OF FERROUS ALLOYS		5. TYPE OF REPORT & PERIOD COVERED Final Report Feb. 1. '73-Sept. 30 '75
		6. PERFORMING ORG. REPORT NUMBER
7. AUTHOR(s) H.R. Larson B.A. Heyer C.P. Biswas		8. CONTRACT OR GRANT NUMBER(s) DAAG46-73-C-0113
9. PERFORMING ORGANIZATION NAME AND ADDRESS Abex Corporation Research Center Mahwah, N.J. 07430		10. PROGRAM ELEMENT, PROJECT, TASK AREA & WORK UNIT NUMBERS D/A Project: ARPA Order 2267 AMCMS Code: 4D10 Agency Accession: DA OE 4735
11. CONTROLLING OFFICE NAME AND ADDRESS Army Materials and Mechanics Research Center Watertown, Massachusetts 02172		12. REPORT DATE August 1976
		13. NUMBER OF PAGES 96
14. MONITORING AGENCY NAME & ADDRESS (if different from Controlling Office)		15. SECURITY CLASS. (of this report) Unclassified
		15a. DECLASSIFICATION/DOWNGRADING SCHEDULE
16. DISTRIBUTION STATEMENT (of this Report) Approved for public release; distribution unlimited.		
17. DISTRIBUTION STATEMENT (of the abstract entered in Block 20, if different from Report)		
18. SUPPLEMENTARY NOTES		
19. KEY WORDS (Continue on reverse side if necessary and identify by block number) Die casting Solidification Ferrous alloys		
20. ABSTRACT (Continue on reverse side if necessary and identify by block number) An experimental ferrous casting machine of 20 lbs. capacity was designed and constructed to evaluate rheocasting and conventional casting processes. This machine is a bottom-pour furnace in which the transfer of the metal "slurry" to the mold was accomplished by pressurizing the furnace chamber and retracting a stopper rod. The melting and casting operation took place entirely under an inert atmosphere at low positive		

DD FORM 1473
1 JAN 73

EDITION OF 1 NOV 65 IS OBSOLETE

UNCLASSIFIED

SECURITY CLASSIFICATION OF THIS PAGE (When Data Entered)

UNCLASSIFIED

SECURITY CLASSIFICATION OF THIS PAGE(When Data Entered)

20. ABSTRACT (continued)

pressure to minimize slag formation. Several problems were encountered during the operation of the furnace and, therefore, the machine was redesigned and modified for more successful operation.

Several experimental models of both conduction and induction type MHD valves were made and it has been demonstrated that some lift can be obtained from these MHD devices to hold the bulk metal and to control its flow but a much stronger lift force would be required for any practical casting machine. Also some improvements have to be made to accomplish surface stabilization of the liquid.

Among all the protective coatings for graphite studied in this work, the most promising approach has been the formation of diffusion bonded metallic carbide on the graphite surface with plasma sprayed zirconia layer as the final mold surface. Hot pressed boron nitride and also silicon nitride have performed fairly well as permanent mold materials.

UNCLASSIFIED

SECURITY CLASSIFICATION OF THIS PAGE(When Data Entered)

1a

FOREWORD

This report covers the complete work done during the contract period February 1, 1973 to September 30, 1975 under the general title "Machine Casting of Ferrous Alloys". The work was carried out at the Abex Research Center, Valley Road, Mahwah, New Jersey 07430 by the principal investigations, H.R. Larson, B.A. Heyer, and C.P. Biswas. The work was sponsored by the Defense Advanced Research Projects Agency under ARPA Order No. 2267 and Contract No. DAAG46-73-C-0113 with Dr. E. Wright and Mr. F. Quigley at the Army Materials and Mechanics Research Center as the program technical monitor.



SUMMARY

An experimental ferrous casting machine of 20 lbs. capacity was designed and constructed to evaluate rheocasting and conventional casting with respect to processing and properties. This machine consists of a bottom pouring induction furnace in which the transfer of the semi-solid metal to the mold was accomplished by pressurizing the chamber and retracting a bottom pouring plug while the stirring paddles were still on. The melting and casting operation took place entirely under an inert atmosphere at low positive pressure to minimize slag formation. Several operational difficulties were encountered during melting and pouring of the melt such as freezing of the melt in the nozzle during pouring, breakage of the stirring paddles and stopper rod, heating of the pressure chamber cover, high resistance to shaft rotation, etc. Therefore, the machine was redesigned and modified for more successful operation. Although the machine was ready for casting, it was decided to discontinue any further work on this machine since our design did not seem to be practical for production scale machine due to its complications in construction and operation.

Several experimental models of both conduction and induction type (and combinations thereof) MHD valves were

made (and proposed) and it has been demonstrated that some lift can be obtained from these MHD devices to hold the bulk metal and to control its flow but a significantly stronger levitation force would be required for any practical casting machine. Moreover, some improvements are necessary to accomplish stabilization of metal-air interface that causes the valve to leak.

For permanent mold application for ferrous casting, coated graphite and some ceramic materials have been studied. For the protective coating of graphite different approaches were taken such as plasma spraying, metallizing, vapor deposition and hot pressing, but most potential approach was the formation of diffusion bonded metallic carbide on the graphite surface with plasma sprayed zirconia layer as the final mold surface. Among all the ceramic materials examined, hot pressed boron nitride and also silicon nitride have shown considerable promise for permanent mold application.

TABLE OF CONTENTS

	<u>Page</u>
Foreword.....	i
Summary.....	ii
List of Figures.....	v
Introduction.....	1
Experimental Ferrous Casting Machine.....	2
Design.....	3
Fabrication.....	6
Operation.....	9
Modifications.....	11
Development of Magnetohydrodynamic (MHD) Valve...	17
Conductive Levitation.....	18
Inductive Levitation.....	22
Induction - Conduction Cells.....	27
Development of Permanent Mold Material.....	30
Graphite.....	30
Ceramic Materials.....	46
Conclusions.....	50
References.....	51

LIST OF FIGURES

<u>Figure</u>		<u>Page</u>
1	Furnace and pressure vessel arrangement.....	52
2	Pressure vessel.....	53
3	Stopper Rod.....	54
4	Drive shaft.....	55
5	Crucible.....	56
6	Stirring paddles.....	57
7	Discharge tube.....	58
8	Abex test bar.....	59
9	Experimental melting and casting unit.....	60&61
10&11	Front and rear view of casting unit.....	62
12	Induction coil with crucible.....	63
13	Refractory components of casting unit.....	63
14	Drive shaft with cooling jacket.....	64
15-17	Shaft actuating assembly.....	64&65
18	Micrograph of conventionally cast and Rheocast 356 aluminum base alloy.....	66
19	Modified crucible.....	67
20	Modified pressure vessel.....	68
21	Stirring rod and assembly.....	69
22	Stirring rod holder.....	70
23	Modified stopper rod.....	71
24	Modified furnace and pressure chamber assembly.....	72&73
25	MHD conduction pump.....	74
26	Theoretical and actual performance of conduc- tion pump.....	75

LIST OF FIGURES - (contd.)

<u>Figure</u>		<u>Page</u>
27	MHD conduction cell electromagnet.....	76
28	Multiple electrode assembly.....	77
29	Rail propulsion conduit and valve.....	78
30	Rail propulsion conduit adjusted for pour up.	79
31	Conduit used as valve for gravity pouring....	79
32	Conical induction coil for levitation.....	80
33	Polyphase levitation pump with Mu-metal flux concentrators.....	81
34	Three-pole, 3-phase levitator for lift and rotation.....	81
35	MHD conduction cell with lower surface stabilized by AC field.....	82
36	MHD induction-conduction cell with lag loop..	83
37	Multiple layer graphite coatings.....	84
38	Micrograph showing the layer of metal under- neath the coating.....	85
39	Dip test experiment.....	86

INTRODUCTION

This is the final report describing the work done at Abex Corporation under a program designed to develop a new technique for a machine casting process that will be practical and economically viable for ferrous alloys. Extensive effort has been conducted in industry prior to this program to develop a ferrous die casting process. All these programs have used existing types of die casting machines (i.e., shot chamber machines of the type used to die cast aluminum alloys). Their development work consisted of (a) minor modifications of the machine or process to permit pouring of steel, and (b) substitution of the shot chamber and die materials that will be more compatible with steel. These programs have not been very successful thus far. The major problem has been the materials that can withstand molten steel. The other minor but still important problems have been casting shrinkage and cracking.

A central concept of this research program is to develop a radically new technology and not make minor modifications of the existing processes. The emphasis of work at Abex was, therefore, on the development of a completely integrated furnace-valve-mold ferrous casting system that will produce quality steel castings in the five to twenty-five pound class more economically than is possible by present casting methods. The system will also produce high

casting speed and employ minimum metal handling. Our efforts have been, therefore, directed in three major areas.

1. Design and fabricate an experimental melting and casting unit capable of examining several casting process possibilities including casting of semi-solid alloys(rheocasting).
2. Determine the feasibility of a magnetohydrodynamic (MHD) valve to control and stop molten metal flow using laboratory scale equipment.
3. Develop a permanent mold for repetitive use in the automatic casting process envisioned.

EXPERIMENTAL FERROUS CASTING MACHINE

The design and fabrication of a pilot melting and casting unit were undertaken with four specific objectives in mind:

1. Evaluation of conventional vs. rheocasting process and development of system parameters for either or both approaches.
2. Determination of the mechanical properties of rheocast metals-cast iron and ultimately steel.
3. Evaluation of the design and materials of construction in the casting unit and the mold, particularly those materials in close proximity to or contact with the molten metal.

- 4 Testing of an MHD valve should it become a feasible device.

Design - The casting unit was designed on the basis of several fundamental requirements of the rheo-casting process as well as other features considered to be generally desirable for a conventional casting process. The following are these basic requirements.

1. The melting and casting operation should take place entirely under an inert atmosphere to minimize slag attack and other problems associated with the presence of an air environment.
2. The melt must be stirred continuously from the point at which the liquidus temperature is reached during cooling to the point at which the casting operation begins.
3. The metal containing some predetermined fraction of solid must be moved rapidly and forcefully from the melting crucible into the mold, maintaining, as much as possible, the stirring action throughout the casting operation.

Figure 1 shows the details of the Abex casting unit that was originally designed to meet these requirements. The materials from which the unit was constructed were as follows:

<u>Component</u>	<u>Materials</u>
Pressure Vessel (Figure 2)	Austenitic stainless steel weld fabrication.
Melting Unit (Figure 1)	Conventional induction melting coils with special support construc- tion for mounting and bottom pour. Power - 100 KW Frequency - 3000 cps Source - MG Set
Bottom Plug (Fig.3)	Alumina
Plug Actuator(Fig.1)	Austenitic stainless steel
Drive Shaft(Fig. 4)	Austenitic stainless steel
Crucible (Fig. 5)	Alumina
Stirring Paddles (Fig. 6)	Alumina
Discharge Tube (Fig. 7)	Alumina

Drive Motor (not shown) Conventional DC motor of 3/4 H.P.

The drive shaft as shown in Figure 4 is water cooled and hence provided with cooling chambers for water circulation. The molds for the casting unit were made of graphite. In order to protect the graphite surface from oxidation and erosion by molten ferrous alloys, the mold walls were first chromized and then plasma sprayed with stabilized zirconia. This coating was selected as a result of our study of permanent mold materials to be discussed later in chapter 3 of this report.

The Abex standard test bars (#D14), shown in Figure 8, were selected for casting to evaluate the performances of the machine and the process. This bar design has been used for many years by the Abex Experimental Foundry for the evaluation of alloys and processes and its foundry characteristics are well documented.

The rheocasting process for the experimental casting unit is as follows:

1. With the chamber open, charge the appropriate alloys to the melting crucible with the paddles in the raised position and the plug in the sealed position.
2. Close chamber and flush with inert gas, nitrogen.
3. Melt down under slight positive pressure of nitrogen gas.
4. Adjust temperature to just above liquidus, lower paddles into melt and begin stirring. The slots cut on the paddles and paddle-to-crucible clearance of 1/4" provide the shear required for rheocasting.
5. Cool the melt to the appropriate temperature below the liquidus corresponding to the fraction solid desired. Since thermocouple cannot be inserted into the metal during stirring, the metal temperature was read from the thermocouple inserted inside the crucible wall. This thermocouple was initially

calibrated against the temperature of the liquid metal inside the crucible and intrapolated to temperatures below the liquidus.

6. Pressurize the chamber to a positive pressure around 30 psi.
7. Pull bottom plug to cast into previously positioned mold. Mold was not evacuated.

This unit can process one 20 lbs. of ferrous casting in each melting and casting cycle.

Fabrication - Figure 9 shows overall views of the casting machine. The pressure vessel or the melting chamber is rigidly mounted on a steel framework at a level that provides sufficient clearance for the mold which was positioned directly under the outlet. The latter is best seen in Figure 10. Manual access to the chamber (other than by unbolting the lid) is through the opening shown in Figure 10 immediately to the left of the name plate. In Figure 11, showing the rear of the chamber, the induction power access port can be seen as well as the over pressure burst disc installation. The presence of this latter safety feature was considered an absolute necessity in view of the unlikely but possible contact of cooling water and molten metal. The disc

was designed to burst at just over 100 psi and provides 1.77 square inches of escape area should the occasion arises.

The induction power access port provides power to a centrally positioned induction coil in the bottom of the melting chamber (Figure 12). The induction coil receives an alumina crucible equipped with an alumina bottom pouring nozzle as shown in Figure 13. The nozzle passes through the bottom of the coil frame and out of the chamber through the bottom outlet shown in Figure 10.

The bottom pouring feature is accomplished by the bottom plug also shown in Figure 13. The taper at the plug bottom fits the taper at the top of the alumina nozzle, thus providing a seal similar to that normally used in small, bottom-pour ladles.

The stirring required by the Rheocasting procedures is to be accomplished by the paddle assembly shown in Figure 13. The paddles used were made of alumina. The rotation of the paddles is concentric with the bottom plug O.D., permitting totally independent operation of both.

The multi-component, water-cooled operating shaft for the paddles and bottom plug is shown out

of the assembly in Figure 14. The shaft consists of a central solid non-rotating bar, which will activate the bottom plug, an axially located tube that provides the paddle drive, and a double-wall axial water cooling sleeve. Figure 1 best shows these details. The shaft was mounted in two bearings that are attached to a vertically movable support beam, and axially aligned exactly with the central axis of the crucible. Figure 15 shows the relationship among these components.

Vertical motion of the paddle assembly, required to move the paddles in and out of the crucible, is achieved by moving the support beam, guided by two guide bars, using the air cylinder shown in Figures 15 and 16. The upper end of the air cylinder shaft is rigidly fastened to the main frame, thus providing vertical motion of the entire support beam.

Rotational motion of the paddles was provided by a motor attached to the rear of the support beam, as shown in Figure 7.

Independent, short vertical displacement of the crucible bottom plug was provided by a manually operated locking lever device not shown here.

Operation - In order to provide a less severe thermal condition for preliminary operations, heats of 356 aluminum base alloy of m.p. 1225°F were made for casting. The details of the first experimental heat are as follows:

Wt. of the charge	- 10 lbs.
Power input for meltdown	- 25 KW
Casting process	- Conventional
Max. temperature of the melt	- 1400°F
Temperature of pouring	- 1350°F
Metal hold time	- 20 min.
Melting & casting atmosphere	- Air
Pouring	- Bottom pour, operated by stopper rod

The major problem encountered in this heat was the freezing of the melt in the nozzle (alumina tube of 0.5" I.D., 1.5" O.D. and 8" long) during pouring. The preheating of the nozzle seemed to be essential to solve this problem. Therefore, a 20 gage Nichrome wire was wound around the nozzle on the outside with a spacing of 6 turns to an inch for resistance heating. A ceramic insulation coating of Ultra-Temp 516 was used to protect the winding. The nozzle temperature was recorded intermittently during the heat.

Using the preheated nozzle, a second heat was made in the same manner as the first one. Just prior to pouring

when nozzle temperature reached about 900°F, the heating coil burnt out and the metal again froze in the nozzle during pouring. The burning was caused by excessive heating of the coil due to high current input (80 volts).

The next step taken was to increase the number of turns to 8 to an inch, use 22 gage wire and apply only 50 volts to the coil. By this a steady temperature of about 950°F was achieved inside the nozzle. A similar heat was made using this preheated nozzle. This time the pouring was successfully accomplished by using a chamber pressure of 5 psi.

A fourth heat was made in which the liquid metal was held in the furnace at 1300°F and the paddles were turned to 100 rpm and the chamber was pressurized to 20 psi. Several leaks in the chamber were detected and they prevented from building any higher pressure. This heat was successful.

The next heat was made for rheocasting. The details are:

Maximum meltdown temperature	- 1350°F
Temperature at which stirring was started	- 1250°F
RPM of the paddles	- 100 (approx.)
Power input during cooling (and stirring)	- 9 KW
Cooling rate during stirring	- 10°F/min.
Temperature of pouring	- 1190°F
Solid fraction at pouring	- 0.5 (approx.)
Nozzle temperature during pouring	- 950°F

This heat was successful. The micrographs of conventionally cast and rheocast 356 aluminum alloy are shown in Figure 18.

Several other problems were encountered during the furnace operations for the above heats. Therefore, it was decided to modify some of the designs to solve these operational difficulties and make the furnace more adaptable to ferrous castings.

Modifications - The problems encountered and the corresponding design modifications made are discussed below.

1. Although calculations have shown that the preheating of the nozzle was unnecessary, the frequent metal freezing became a serious problem during pouring. This was probably due to slow leakage and subsequent freezing of the metal in the nozzle during melting and stirring of the melt. In any case, it was decided to enlarge the nozzle diameter and preheat the nozzle to about 2600°F for ferrous castings. But, by using a resistance heating coil, a maximum of only 1200°F was reached in the nozzle. Therefore, an induction heating was employed. Due to poor magnetic permeability of alumina nozzles, iso-

pressed high density alumina graphite refractory nozzles were used instead. This is a proprietary material made by Vesuvius Crucible Company and is supposed to have higher resistance to oxidation and erosion by metal than pure graphite has. For convenience, the crucible and the nozzle were made of one piece as shown in Figure 19.

An induction coil of 5-1/2" diameter and 6" length was used for preheating the nozzle. Since both the melting coil (for the crucible) and the heating coil (for the nozzle) were required to run at the same time and the power input in these two coils could not be controlled independently from the same power supply (the power drawn by each coil is dictated by the degree of magnetic coupling in the coil), a separate power source (15 KW, 3,000 cycles MG set) was used for the heating coil. Since it is convenient to enclose the heating coil in the furnace chamber, the pressure vessel was redesigned to accommodate the heating coil as shown in Figure 20.

2. Excessive leakage through several connections to the pressure chamber prevented building up of high pressure in the chamber. Use of better seals improved this pressure build-up. It was

found that a pressure of 20 psi in the chamber was sufficient for successful pouring during rheocasting of up to 0.6 solid fraction. Therefore, the modified stainless steel chamber was rated for only 30 psi.

3. The lid of the pressure chamber appeared to be heated up by the radiation of heat from the molten metal. Since this heating could be severe during processing of ferrous metals, it was decided to water cool the lid. A water cooling jacket made of stainless steel was welded on the outside of the lid, as shown in Figure 20.
4. The high purity slip-cast alumina paddles supplied by Norton Company was found to be unsuitable due to their insufficient strength - there was frequent breakage problem. In their place, a set of closely spaced cylindrical alumina tubes was used for stirring the melt. These tubes are made by McDanel Refractory Company and used for thermocouple protection tubes. In case of their failure, silicon-oxy-nitride paddles (made by Norton Company) would have been used instead. Since these stirring tubes undergo severe stress during stirring and their strength drops drastically around 2000°F, cylindrical graphite rods were inserted inside the tubes for reinforcement. The graphite rods were fastened to the

stirring rod holder and the alumina tubes were cemented on to the graphite rods as shown in Figures 21 and 22. The exposed graphite surface was given a protective coating to resist oxidation.

5. In one case the stopper rod broke during the melt-down period. This was caused by the expansion of the plug shaft since it was rigidly fixed at the top end by a push-pull clamp device. In order to allow for its free expansion, the plug shaft was later attached to the push-pull clamp through a flexible connector. By this arrangement the stopper rod closed the nozzle by the weight of the shaft and for pouring, it was pulled up by the clamp.

The stopper rods were also replaced by McDanel's alumina tubes as shown in Figure 23. These hollow tubes were filled with refractory packing.

6. The resistance to shaft rotation was found to be high. This was due to the shaft not being perfectly straight and also the improper mounting of the stationary water jacket around the shaft. This problem was solved by improving all the shaft bearings and redesigning the water jacket support system.

7. There was an occasion of rise of the liquid metal in the clearance between the center shaft (for operation of stopper rod) and outer shaft (for rotation of the paddles) by capillary action. This was caused by an excessive rise of the meniscus of the liquid metal during meltdown. The entire shaft assembly was, therefore, raised about 3" to prevent any metal contact. This also brought the paddle holder outside the induction coil and prevented its unnecessary heating by the induction field. This also necessitated longer stopper rod and stirring rods.
8. The assembly for lifting the pressure vessel cover and the shaft was modified to provide a smooth lift with adjustable speeds and also to hold the cover and the shaft in any intermediate position. A larger air cylinder was installed and also the brass bushings were replaced by linear ball bearings for the sliding shafts.
9. A second sight port was installed on the pressure vessel lid for lighting the inside of the vessel. (See Figure 20).
10. Three guide rods were provided on the pressure vessel to guide and align the vessel cover. (See Figure 20).

11. One relief valve was installed in the pressure chamber.
12. Provisions were made for independent lifting of the cover, shaft and plug rod.
13. One thermocouple was installed inside the nozzle wall to record the nozzle temperature.

An overall view and a schematic drawing of the modified furnace assembly is shown in Figure 24.

All the modifications were completed and the machine was ready for casting. The level of confidence for successfully producing experimental castings from the machine was high. However, after discussing the long term potential for developing a full scale production process using the same approach, it was decided that further work would not be in the best interest of the objectives of the overall program. Material and mechanical complications, not envisioned at the outset of the program, strongly indicated that this approach should be abandoned in favor of other approaches then under consideration by other contractors.

It was disappointing to have placed the technical effort into the Experimental Casting Machine and to abandon it before producing even one ferrous casting. However, the decision was recognized as being in the best interest of the overall program.

DEVELOPMENT OF MAGNETOHYDRODYNAMIC (MHD) VALVE

This phase of the ferrous casting program calls for the investigation to determine the feasibility of using magnetohydrodynamic force as a valve to control and stop molten metal flow. This electromagnetic valve would circumvent many of the mechanical and material problems associated with existing pouring methods such as stopper rod valve, slide gate valve, etc.. The control or complete stoppage of flow can be accomplished by the magnetohydrodynamic countering of the force of gravity. The basic force in an MHD device can be expressed by

$$\vec{F} = \vec{J} \times \vec{B} \quad (1)$$

where F is the force experienced by the liquid

J is the current density

B is the magnetic flux density.

There are two kinds of MHD device of interest, (a) conduction type and (b) induction type. In the conduction device, a direct current is applied through the liquid (in addition to a magnetic field applied in a direction perpendicular to that of the current), whereas, in the induction device, the current is induced in the liquid by an external induction field.

In a conduction cell the static support of a vertical column of liquid against the gravity is given by the relation,

$$JB = pgh \quad (2)$$

where p is the mass density of the liquid

g is the acceleration due to gravity

h is the height of the liquid column

In an induction cell, on the other hand, the static re-support of a liquid column is given by,

$$B^2/2\mu_0 = pgh \quad (3)$$

where $\mu_0 = 12.57 \times 10^{-7}$ in MKS units.

On the basis of Equations 2 and 3, calculations have shown that the suspension of a sizeable head of molten iron is feasible by using magnetohydrodynamic forces. In the preliminary experiments of both conduction and induction type MHD valves of laboratory model, it was found that a reasonable lifting force could be generated by the MHD device but the major problem was the instability of metal-air interface, and therefore, a tendency for the valve to leak. The details of these experiments are discussed below.

Conductive Levitation - The set up for the conduction type experiment is shown in Figure 25. It consists of a plexiglass U-tube with a conduction pump installed in one leg. The cross section of the cavity is rectangular with 1.5" x 0.05" sides. Mercury was used as the liquid medium. Currents varying from 0 to 150 amps were applied along the long sides of the cavity and a

magnetic field of about 2,000 gauss was applied by a permanent magnet along the short sides. The MHD force generated thereby was vertical and was computed by measuring the difference of the mercury levels in the two legs.

The MHD force generated was found to be proportional to the applied current as shown in Figure 26. The graph also shows the theoretical force that was calculated on the basis of uniform current and flux density. The discrepancy is probably due to fringing of the electrical and magnetic fields leading to non-uniform field densities and also energy lost due to heating of mercury. This heating was, fortunately, very minor.

The stability of the mercury-air interface was investigated by attempting to pump the mercury above as well as below the electrode contacts. In both cases the liquid surface was unstable.

It was realized from this experiment that a stronger magnetic field was necessary for levitation of any practical importance. Therefore, an improved conduction cell was built (Figure 27) in which an electromagnet capable of producing 4,000 gauss field and a circular cross section tube with round insertable multiple electrodes (Figure 28) were used. The circular geometry was selected because of its conformity to a practical refractory nozzle. The test

of this apparatus indicated no appreciable difference in the lift obtained in the first experiment. This was due to considerable power loss in the electromagnet structure and, therefore, its inability to attain the design value of magnetic flux. The current required was approximately 40 amps per c.c. of mercury with 3.7 watts per c.c. at the electrodes.

Besides being insufficient the levitation force was also non-uniform in the liquid due to the discrete electrodes in this device. Therefore, a pair of long rail electrodes in combination with a pair of long electromagnetic poles were used to form a rail propulsion device. This is shown schematically in Figure 29. The molten metal is confined in the space between two conductive rail bus bars contacting the liquid and two long magnetic poles. When the current and the magnetic field are applied, the liquid experiences propulsion force along its entire length.

The electrodes were made hollow for cooling by the circulation of suitable coolant. The electrodes can be made of the same metal as the liquid in which case the electrodes become consumable but the extent of their melting can be controlled by controlling their cooling rate. The electrodes can also be made of any conductive

material of higher melting temperature and a conductive refractory coating can be used on the electrode to protect from any corrosion or erosion. Alternating current may be used in place of a steady current provided the phase relationship between rail current and magnetic field is time invariant. If the cross section of the nozzle is made uniformly tapered toward the exit end, the magnetic field will be more concentrated near the exit end, thus providing a surface stabilizing action on the terminal liquid surface.

Figures 30 and 31 show our laboratory model of rail conduit hinged to the bottom of a furnace through a cylindrical gate valve. The conduit can be set at different angles with the furnace so that both pouring up and pouring down are possible. In our experiment with liquid woods metal, a metallostatic head of about 5" was supported by applying 150 amp current and 1 kilogauss magnetic field. It was calculated that 10 amp per cm^2 per gm per cm^3 per kilogauss is required to balance any conductive medium against gravity.

Therefore, a much stronger current and magnetic field are required in our model rail device to hold a vertical column of any practical importance. It is worth mentioning that the above rail propulsion device can also be used for molten metal conveyance as an alternate to the existing linear induction motor devices.

Inductive Levitation - Inductive levitation relies upon the coupling of energy from a primary coil into the melt as a one-turn secondary. In the induction type experiment woods metal was used in a 0.5" diameter pyrex tube. The current was supplied from a 10 KW, 610,000 Hertz power source into a 6-turn induction coil placed around the tube. Although the MHD force supported a small column of liquid, the metal trickled through at the center. The leak was probably due to the absence of any vertical force at the center. Therefore, for an efficient lifting of the liquid throughout the cross section we need an induced magnetic field that will produce stress fields with strong vertical components at all points. This can be achieved by using a conical induction coil that is capable of producing magnetic fields with strong horizontal components at each point in the liquid. The achievement of levitation has been obtained in the past through use of this type of tapered coil configurations.

Accordingly, we built a conical levitation coil assembly as shown in Figure 32. A copper plated ping pong ball was initially used for levitation. When resonated with 0.01 mfd at 17 kHz, the heating of the plating occurred without any levitation. No levitation could be achieved up to 150 volt-amp power. Aluminum

and copper discs and hoops of 1" to 1-1/2" diameter were also tried for levitation, but the coil either propelled or turned them on their ends, but did not hold them levitated.

Besides generating a magnetic field with strong horizontal component, the magnitude of induced current and its penetration depth are equally important for successful levitation. These factors are governed by the frequency of the power supply. A higher frequency field generates a stronger eddy current, shallower skin depth and consequently more heating and less levitation of the melt. An annular channel will have higher levitation efficiency than a solid cylindrical channel. The partitioning of levitation and heating is also influenced by the power factor. The primary coil can transfer maximum current for a given voltage when it is tuned for unity power factor. If the secondary is assumed to be reactive, its current will be 90° out of phase with primary current and there would be no levitation. If the secondary is also tuned to resonance, a tremendous current would flow and there would be no induction heating because resistance is zero, yet, there would be levitation because the currents are phased. There apparently can be levitation without heating (at least cryogenically).

But how do you tune a slug secondary? Furthermore, the tighter the coupling (closeness to unity) the greater the mutual interaction between the coils and, therefore, they cannot be tuned independently.

For successful levitation, it is necessary to generate a large gradient of the magnetic field because the levitational force is proportional to and in the direction of the negative gradient of this field. This gradient field can be achieved by the divergent end effects in an induction coil. But this diverging magnetic field, while necessary, is not sufficient for the stable operation of the MHD valve which must be a servo system. By combining paired static levitation coils in a polyphase linear stator, wherein the molten charge in the nozzle will be a liquid rotor, we can obtain an MHD valve system adapted to treatment by servo theory.

The arrangement is shown in Figure 33 where coils are stacked axially to comprise a travelling wave stator coil of a linear motor. Interference with spatial wave length caused by coil dimensions in the stator system was solved by using mu-metal flux concentrators in our experimental model. Each coil is comprised of a mu-metal cup-core flux concentrator completely filled with a coil, except for a central bore. The mu-metal cores, when stacked, nest together to form a low reluctance magnetic path and an

aligned bore. Coils, available in sets of three, have 15 turns of 1/8 inch copper tubing or 150 turns of No. 18 enamelled wire. A 3-phase automobile alternator was modified and used as the power source. Unfortunately, only 225 volt-amperes could be generated by this alternator in each coil type. The coils were connected across A, B and C phases respectively for 3-phase levitation or an A, -B and C connection for a partial, derived 6-phase connection. The latter connection gives most efficient pumping.

Because of the power limitation of our 3-phase generator and the inability to tune the equipment, levitation only sufficient to raise solid conductors was achieved. When an iron core was added to the stator very strong levitation and propulsion of aluminum tubing was obtained. Our model had a 150 to 1 turns ratio or a 15 to 1 turns ratio depending on the coils used. Since the molten charge is one shorted turn, the induction efficiency is very low. A practical MHD valve without iron flux concentrators must, from the standpoint of spatial frequency dimensioning, be a single layer solenoid. The fundamental problem is that of satisfying the contradictory requirements of making the volts-per-turn in a single layer primary sufficiently high to ensure sufficient eddy

current induction in the melt for efficient levitation force. This requires tuning the levitation coils to resonance and the volts-per-turn of coil not to be reduced by the loading of the melt below an efficient levitational value.

Another method of levitation was also investigated. The model is shown in Figure 34. This model combines a rotating field with an ascending travelling wave. A vortice pump is not the object here. Under slip conditions the levitation forces on a liquid would be static and hopefully will stabilize the lower suspended surface. Lovell⁽¹⁾ first suggested the rotating levitational field and Wroughton⁽²⁾ et al described its use for levitational melting and in connection with surface stabilization stated: "The resultant rotative fields, if multiple phase power is used, conserves energy by reducing the effect of the weak spot or "hole" in the magnetic field through which the molten metal sometimes tends to be discharged.....effective rotation due to the phase differences will tend to prevent discharge of molten metal from the field when it is operated just above the value needed for discharging the melt in order to conserve the energy". In the case of our model as applied to the MHD valve, the rotating field is the 3-phase

equivalent of the single-phase ferrite stabilizer as will be suggested later as our stabilizing approach. The stabilizer has circular symmetry, the rotation of which will provide an induced surface tension reinforcing field which will smear the lower surface with "wiping" forces. The surface will probably not rotate due to friction with the nozzle wall. Some levitation has been achieved with this device but not enough for practical applications.

Induction-Conduction Cells - Since it has been observed in our experiments that a conduction cell is more efficient in levitating liquid than an induction cell, our next approach was to use a combination of conduction and induction cells in which most of the lift would be provided by the conduction cell while the induction field would stabilize the liquid surface and provide some lift. A schematic diagram of the experimental arrangement is shown in Figure 35. In this case the liquid-air interface is stabilized by the application of an RF field producing a transverse magnetic field with a strong gradient.

Experiments were carried out with the fringing field of a rectangular ferrite core and the results showed that sufficient fields could be produced without difficulty to levitate small copper and brass specimens,

but mercury and steel will require further effort. At 20 kHz, only the large pieces would levitate; as the frequency was increased, the smaller sizes would float up. The mercury presented a problem because of its high density, and required much higher field gradients. The steel appeared to be just below the levitating points as the frequency was raised to 50 kHz, but the breakdown voltage of the capacitors was reached at this point. It seemed likely that an improved larger core with suitable gap dimension and a strong field gradient would be necessary for the stabilization of mercury-air interface.

An alternative valve design was also proposed and it is shown schematically in Figure 36. A conduction pump of circular channel having inserted cylindrical electrodes would provide an accelerator to hold back most of the head pressure. Around the lower meniscus of the liquid metal column would be a cup-core coil structure comprising a primary coil and a lag loop coil for interface stabilization. While only one coil element is shown having a lag loop, to comprise a single phase levitator, two or three such coil sections might be employed to expand to a two or three phase pump.

The work on the development of MHD valve was discontinued at this point because the entire effort of this project was directed in the development of ferrous casting machine.

DEVELOPMENT OF PERMANENT MOLD MATERIAL

The development of permanent mold is essential for making any casting process rapid and economical. We selected graphite and some ceramic materials for potential permanent mold application.

Graphite - Graphite has been considered by us to be the most suitable permanent mold material because of its low cost, easy machinability and above all its excellent thermal shock properties. The latter is particularly important in our ferrous casting system because of high casting temperatures involved. The thermal shock resistance of a material is expressed by the parameter μ as,

$$\mu = \frac{KS}{\alpha E}$$

where K is thermal conductivity

S is tensile strength

α is coefficient of thermal expansion and

E is modulus of elasticity .

The higher the value of μ the better is the thermal shock resistance and graphite has higher μ than any other permanent mold material, both refractory metals and ceramic materials.

The main problem with the graphite is its poor resistance to oxidation and erosion by molten ferrous alloys. Therefore, our primary effort was devoted to developing a coating that will protect the graphite surface.

It has been observed in our previous works that the failure of all types of graphite protective coating occurs primarily by (a) cracking and (b) spalling or peeling. These are caused mainly by the following factors:

1. poor bond between the coating and graphite,
2. difference in the coefficients of thermal expansion of the coating and the graphite,
3. oxidation of graphite underneath the coating.

On the basis of these above factors the following graphite coatings were selected for evaluation:

1. Proprietary coating
 - a. Ultra - temp 516
 - b. Graphi-bond 551R
2. Plasma sprayed refractory oxide coating
3. Plasma sprayed refractory oxide coating chemically bonded with refractory particles mixed with the graphite
4. Diffusion bonded carbide coating with plasma sprayed refractory oxide layer as the final surface
5. Diffusion bonded carbide coating with diffusion bonded oxide layer as the final surface.

The types of graphite that were selected to evaluate different types of coating are:

- a. conventional graphite of varying coefficient of thermal expansion of the following types:
 - i) extruded graphite from Union Carbide Co. (ATJ, ATL and AGSR grades)
 - ii) molded graphite from Great Lake Carbon Co. (MHLM grade)
- b. Unicast molded-to-shape graphite from Unicast Development Corporation.

Before any coating was applied, the graphite surface was sand blasted lightly with 80 mesh alundum particles to achieve some mechanical bond with the coating. The surface was then cleaned by heating the graphite to about 350°F and quenching in boiling water for about 2 min. Finally, it was dried in oven at 300°F for about 30 min.

A simple mold was designed to evaluate most of the coatings under actual casting conditions. The mold had a rectangular cavity of about 15 lbs. casting capacity. Graphite formed the drag while the cope was made of sand. A simple step was provided on the graphite surface to test how well the coating adheres to the corners. All the castings were made of various ferrous alloys poured between 2300°F and 2800°F.

A detailed discussion of the coatings and the test results are given below.

Proprietary coating

Ultra-temp 516 coating - This is a proprietary coating made by Aremco Products, Inc., N.Y. This material is a high strength zirconia base ceramic adhesive (heat cure) that can presumably withstand temperatures up to 4400°F. The coating was applied by brush in thin coats several times, each coating being followed by curing at 200°F for 2 hrs. The coating started to crack in some areas during curing and also some reaction was observed in the coating during pouring of the metal.

Graphi-bond 551R coating - This is also a proprietary coating made by Aremco. This is a graphite base adhesive that can withstand temperatures up to 5400°F in a reducing atmosphere. The coating was applied by brush in a thin layer and cured at 250°F for 3 hrs. After about eight castings the coating started to appear spongy indicating either oxidation or reaction with the metal has started.

Plasma sprayed oxide coating - On the basis of earlier works at Abex, alumina (Metco 101) and magnesia stabilized zirconia (Metco 210-NS) were considered

to be the best coating materials because they are thermodynamically most stable oxides and chemically most non-reactive to ferrous metals. We have examined:

- a. single layer
- b. double layer and
- c. four layer graded coating.

- a. A single layer coating of thickness about 0.006" was applied on the graphite surface by plasma spraying at 75 volts and 400 to 500 amps using Metco gun. The spray distance was 4" and nitrogen flow rate of 90 CFH, hydrogen flow rate of 20 CFH, carrier gas flow rate of 400 CFS and powder feed speed dial setting of 20 to 70 were used.

A visual examination of the graphite surface after the first casting showed that the coating spalled off in the gating area where the metal first hit the mold surface.

- b. The above failure was believed to be due to poor bond between the coating and graphite. Therefore, the bond was improved by using a bond coat of NiAl (Metco 404) on the graphite surface. The bond coat thickness was about 0.002". This produced a slight improvement, the coating started to fail in the gating area after 2 to 3 castings.

- c. Since NiAl and MgO-ZrO₂ have different coefficient of thermal expansion, it was then decided to use compensating layers between the bond coat and the final coat to absorb the thermal stress. Two compensating layers were used (Figure 37), the first one consisting of a mixture of 65% NiAl and 35% MgO-ZrO₂ (Metco 413) and the second one comprising of a mixture of 35% NiAl and 65% MgO-ZrO₂ (Metco 412). The thickness of each of these compensating layers was about 0.002".

This four layer graded coating produced a great improvement. The coating lasted for about 12 castings after which the peeling of the graphite surface was noticed in the gating area and also near the edges of the step that was provided on the graphite surface. The peeled off layer was examined under microscope and was found to consist of a layer of about 0.015" thick metal underneath the coating as shown in Figure 38. It appeared that the metal penetrated the coating at cracks and spread underneath it. The void between the coating and graphite was perhaps produced by oxidation of the graphite surface.

Plasma sprayed coating on ceramic infiltrated graphite - Our next approach was to improve the bond between the graphite and coating by mixing graphite with refractory particles of the same composition or other that is capable of forming chemical bonds with the coating material so that the coating will be fusion bonded with these particles during plasma spray.

There are several companies that manufacture Al_2O_3 mixed graphite. We examined one sample from Vesuvius Crucible Company and the material was found to be not strong enough to be used as permanent mold material. This poor strength was probably due to poor bond between the graphite and Al_2O_3 particles.

We contacted Unicast Development Corporation of New York who has a proprietary method of making molded-to-shape graphite. They proposed that their technique might be able to produce a strong graphite refractory composite and the following three composites were made:

- a. NiAl mixed graphite
- b. Al_2O_3 mixed graphite
- c. $\text{MgO} - \text{ZrO}_2$ mixed graphite

About 10 to 12 volume pct of the refractory particles of size $-170 + 10\mu$ was mixed with graphite in each

case. But, these graphite specimens also exhibited poor strength and durability. Moreover, the graphite surface had a powdery appearance that prevented any adherence with plasma sprayed coating.

Diffusion bonded carbide coating with refractory oxide coating as the final surface - One of the problems associated with the plasma sprayed coating is its inability to wet the graphite surface adequately and thereby produce a good bond. Therefore, it was decided to change the graphite surface chemically so that the subsequent ceramic coating will have a better adherence. The most convenient method was to form metal carbides on the graphite surface since carbon has good diffusivity in most of the metals. The procedure is to deposit a thin metallic layer on the graphite surface and then form carbide by diffusion annealing. By this the carbide layer will be diffusion bonded to the graphite. From thermodynamic considerations we selected the following three carbides:

- a. Chromium carbide
 - b. Titanium carbide
 - c. Molybdenum carbide
- a. Chromium carbide - The chromizing of graphite samples was done by pack metallizing technique

at the Chromally Research, New York. The coating thickness was about 1 micron (4×10^{-5} in.). After diffusion annealing at 2000°F for 1 hr. in a vacuum surface, the graphite surface was found to contain Cr_{23}C_6 by x-ray diffraction technique (see Table 1). Two samples were prepared, one of them was coated with a single layer of MgO-ZrO_2 (applied by plasma spray) while the other was coated with 4 layer graded MnO-ZrO_2 (Figure 37) using NiAl as the bond coat on the carbide surface.

Table 1

Results of X-ray Diffraction Analysis

<u>Coating Before Diffusion Annealing</u>	<u>Surface Constituents</u>
Chromium by pack metallizing	Cr_{23}C_6
Titanium by pack metallizing	TiC - Major
	TiN - Major
	C - Major
	TiO_2 - Minor
Titanium by vapor deposition	C - Major
	TiO_2 - Minor
	Ti_4O_7 - Minor
Molybdenum by plasma spray	Mo - Major
	MoC - Minor
	γ - MoC - Minor

For evaluation of these coatings we used dip test instead of pour test since dip test is faster and less expensive. Although dip test and pour test are not identical for mold evaluation, the thermal shock resistance and mold-metal reaction can be evaluated equally in both the tests. However, in our case the dip test was used only for screening purpose. The best coating was used in actual mold for pour testing for final evaluation. Cylindrical samples of 2-1/2" dia. x 8" length with insertable steel rod at one end was prepared for the dip test. The test arrangement is shown in Figure 39 where A is an induction furnace containing molten cast iron (C-3.5% and Si-2.00%) at a constant temperature of 2350°F with power on, B is a cylindrical steel chamber with the bottom open and top covered with a transite lid, C is the cylindrical specimen that is suspended by a handle bar at one end and inserted into the chamber through its lid, and D is the gas port that leads argon gas into the chamber to flush it continuously. This inert atmosphere was maintained to prevent any slag formation. A gap of about 2" was provided between the metal surface and the bottom of the chamber for the outlet of argon. The

specimen was dipped into the metal by about 5" and held there for several seconds until the surface reached the temperature of the melt. It was then pulled out and allowed to cool to about 1000°F and then dipped again. This cycle was repeated 10 times before it was cooled to room temperature for visual examination. The results of the dip tests are shown in Table 2. As can be seen the 4 layer graded coating of MgO-ZrO_2 survived 50 cycles of dip test whereas the single layer coating started to fail after about 40 cycles.

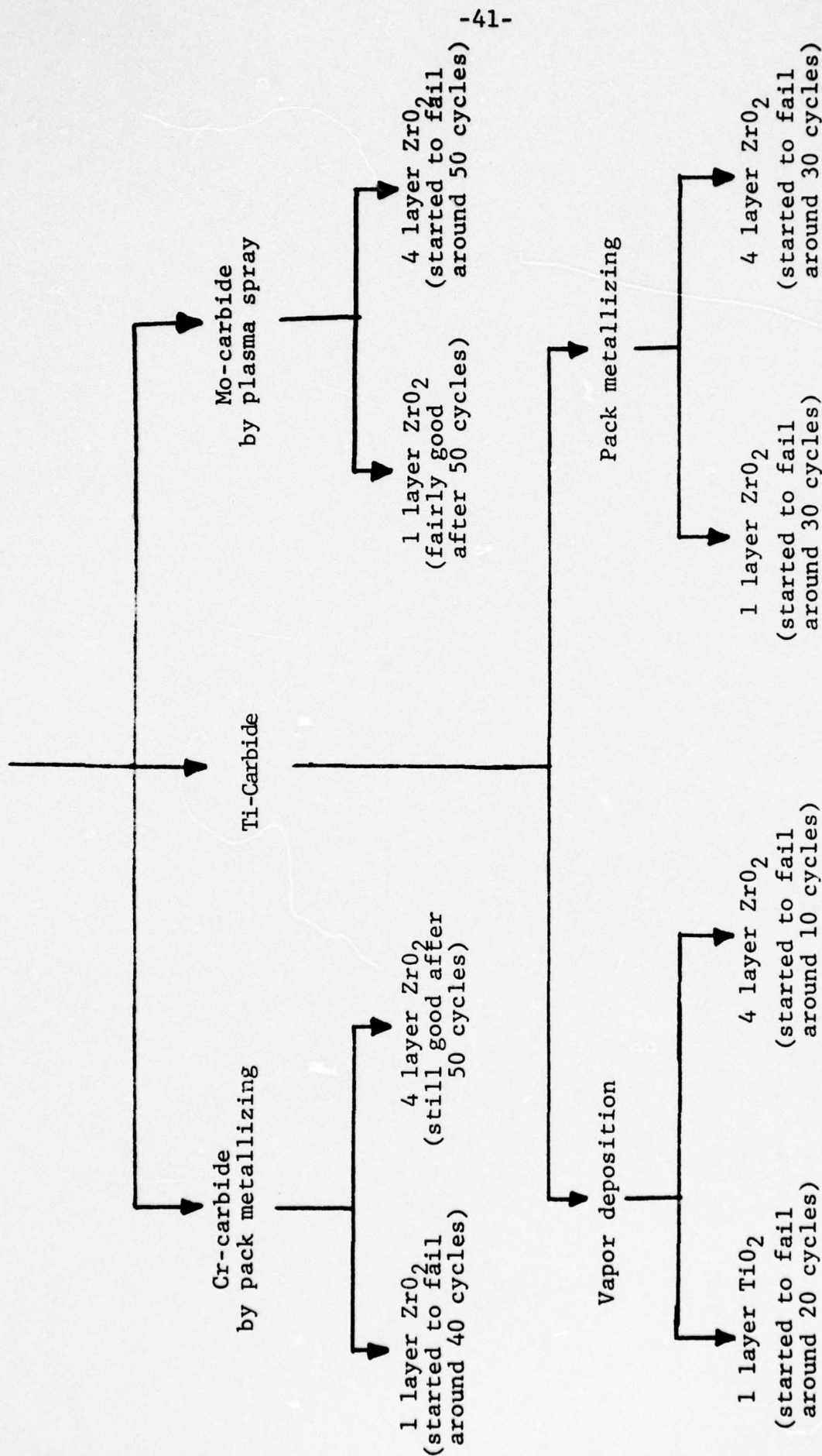
The specimen with four layer graded coating was later dip tested in liquid steel at 2950°F, but after about 3 cycles the coating started to fail. The failure seemed to have occurred due to partial melting of NiAl . The melting point of stoichiometric NiAl is only 2980°F and our NiAl powder contained off-stoichiometric composition of lower m.p.

- b. Titanium carbide - Several procedures for coating graphite with titanium were investigated of which the following two methods were selected:

- i) Vapor deposition
- ii) Pack metallizing

Vapor deposition of titanium was done at AMMRC (Army Materials and Mechanics Research Center), Massachusetts

DIFFUSION BONDED CARBIDE COATING



by vaporization of pure titanium wires under vacuum. Pack metallizing was done by Chromally Research, New York by packing graphite specimens with titanium powder and carrier gas in a closed crucible and heating at around 2000°F inside a furnace. The coating thickness in each case was about 1 micron. The specimens were diffusion annealed at 2000°F for 1 hr. in a vacuum furnace and the results of x-ray diffraction analysis of the surface are shown in Table 1. As can be seen the vapor deposition technique was not successful due to formation of excessive oxide and no carbide. Moreover, it is an extremely slow process. In titanizing process, however, there was formation of some TiN along with TiC on the surface. The appearance of strong carbon lines in the diffraction pattern indicates that the carbide layer was very thin. Several experiments were run to minimize the formation of TiN but were not very successful. Since TiN has a very high melting point we considered its presence to be not harmful. Two samples were prepared by vapor deposition technique, the one coated with single layer TiO_2 lasted about 20 cycles and the other one coated with 4 layer graded MgO-ZrO_2 lasted only 10 cycles. On the other hand, two samples were prepared by pack metallizing technique, one was

c. Molybdenum carbide - Since no successful pack metallizing process exists for molybdenum so far, it was deposited by plasma spraying (about 0.001" thick) and molybdenum carbide was formed by diffusion annealing at 2000°F for 1 hr. in a vacuum furnace. The plasma spraying of Mo was done in the air since the extent of oxidation of Mo during plasma spraying was only about 5%. The x-ray diffraction analysis showed that the conversion of Mo to its carbide (Table 1) on the graphite surface was difficult by diffusion annealing.

Both the single layer MgO-ZrO₂ specimen and 4 layer graded MgO-ZrO₂ specimen lasted about 50 cycles of dip test. These specimens were later dip tested in liquid steel at around 2950°F and the coating started to fail after about 3 cycles. This failure appeared to be due to melting of the bond coat NiAl. Therefore, the 4 layer graded MgO-ZrO₂ coating on Cr-carbide surface performed best in the dip test. This coating was subsequently evaluated by pour test in graphite molds since dip test was a severe test and in actual casting conditions the maximum temperature the graphite mold wall reaches is substantially less than that of the liquid metal. Small pig molds of graphite with 5"x3"x2" mold cavity were made and the entire surface was chromized by pack metallizing technique. An x-ray diffraction

analysis revealed that Cr_{23}C_6 was already formed on the graphite surface by the metallizing treatment. Therefore, no diffusion annealing was done for these molds. One mold was given a coating of MgO-ZrO_2 with a bond coat of NiAl whereas the other was given four layer graded MgO-ZrO_2 coating using NiAl as the bond coat. During plasma spraying some problems were encountered, an excessive amount of coating material was found to accumulate around the corners leading to a non-uniform coating in these areas. Liquid steel was poured in the mold cavity at around 3000°F and after about 3 castings the coating started to spall around the corners in both the molds. The coating seemed to have separate at the Cr_{23}C_6 - NiAl interface, It is likely that during plasma spraying of one side of the mold cavity, the adjoining sides received some "overspray" which was normally not very adherent and this resulted in a failure of the coating in these areas.

Studies were made to see if the castings could be made against the chromized surface without using any subsequent plasma sprayed coating. Although Cr_{23}C_6 is dissolved in liquid steel to some extent, it is possible that the metal next to the mold surface might solidify immediately on contact with the mold wall (except in the gating area) and cause negligible amount of mold erosion. But the coating failed after about 6 castins due to the coating-to-metal reaction.

Pour test was also conducted on titanized (by pack metallizing) and plasma sprayed surface. Since x-ray diffraction analysis of the titanized surface showed the absence of any residual titanium, no diffusion annealing was performed on these titanized molds. Two molds were titanized, one was coated with MgO-ZrO_2 using NiAl as the bond coat and the other with four layer graded MgO-ZrO_2 . The plasma spraying was done carefully so that no additional deposit from "overspray" is formed. The coating in both the molds lasted for about 10 castings before the corners started to spall. It seemed that the coating life can still be enhanced by careful plasma spraying.

Diffusion bonded carbide coating with diffusion bonded oxide layer as the final surface - The next step taken was to improve the bond between the carbide surface and the oxide coating by forming diffusion bonds between the two (Figure 37). This was accomplished by plasma spraying a pure metal on the graphite surface and then diffusion annealing in a controlled oxidizing atmosphere. A diffusion bonded carbide layer was formed at the graphite surface and a diffusion bonded oxide layer on the carbide surface to form the final surface. From thermodynamic considerations titanium was selected as the coating material. Pure titanium powder was plasma sprayed under vacuum (done by General Plasma Associates, Conn.) to a thickness of about 0.01" on the graphite surface and the

carbide-oxide layers were formed by diffusion annealing the specimen at 1400°F for 4 hrs. in a controlled oxidizing atmosphere. The evaluation of these specimens was not completed before termination of the project.

Ceramic Materials

Besides graphite, the following hot pressed ceramic materials were also studied for permanent mold application:

- a. Silicon nitride (from Norton Co.)
- b. Zirconium diboride (from Carborundim Co.)
- c. Boride "Z" (" " ")
- d. Boron nitride (" " ")
- e. Modified ZRBSC-D (" Norton Co.)

All these materials were evaluated by pouring ferrous metals in the temperature range of 2400°F to 2700°F in open ended cylindrical sand molds using these specimens as chill plates. Zirconium diboride and boride "Z" specimens were small and they were embedded in a sand mold of simple rectangular cavity. No preheating of the specimens were done. Some of these materials were tested in both coated (with single layer MgO-ZrO_2) and uncoated condition but the coating in each case started to fail within 5 castings. Silicon nitride (uncoated) showed an

extremely slow reaction with the metal before it shattered into pieces during the eighth casting indicating its insufficient thermal shock resistance. Zirconium diboride showed an extremely poor thermal shock resistance and cracked during every pouring. Boride "Z" showed some cracking and reaction with the metal. Boron nitride showed good results; although it showed slight reaction with the metal, it did not crack at all in a total of 16 castings.

ZRBSC-D is a hot pressed ceramic mix of zirconium boride and silicon carbide that is capable of withstanding high temperatures. The thermal shock resistance of this material is presumably very good but it has been demonstrated in other works that the material shows some reaction with the ferrous metals. Therefore, two different modifications were made to reduce the mold-metal reaction,

1. mixing of CaO stabilized ZrO_2 with ZRBSC-D
2. hot pressing a surface layer of CaO stabilized ZrO_2 on ZRBSC-D.

Three different mixes were tried, 29, 19 and 13 vol. pct. of CaO- ZrO_2 , to reduce the mold-metal reaction without impairing its thermal shock resistance. Circular discs of 4" dia. and 3/4" thick were made. On

examining these samples in the as-pressed condition it was found that the disc with 29% CaO-ZrO_2 was very seriously crazed cracked probably due to significant shrinkage because of reaction of zirconia with the balance of the mix. However, all the discs cracked immediately after the metal was poured suggesting their very poor thermal shock resistance for our application.

Since mixing of zirconia was contributing to the poor thermal property, attempts were then made to hot press thin layers of graded CaO-ZrO_2 on ZRBSC-D surface. A three layer graded coating of increasing CaO-ZrO_2 content (each layer of about 0.003" thickness) was originally planned to compensate the difference in the thermal expansions of the substrate and zirconia, but this could not be accomplished by Norton's existing facilities. Instead, just one layer of CaO-ZrO_2 of about 0.03" thick was hot pressed on ZRBSC-D substrate.

Problems were encountered in selecting the hot pressing temperature because of large difference in this temperature for CaO-ZrO_2 and ZRBSC-D. However, the problem was finally resolved and two hot pressing temperatures were selected. When cooled to room temperature after hot pressing, the samples showed numerous cracks in the zirconia surface layer probably because of difference in the thermal contractions of the substrate and

the surface layer. The surface layer was ground off from the substrate and an x-ray diffraction analysis of this layer showed some preferential diffusion of ZrB_2 into CaO-ZrO_2 . It was noticed during surface grinding that the bond between the substrate and the surface layer was very good in some areas and poor in others. However, considering the difficulties encountered in hot pressing operation and the cracking problem of the surface layer, this concept was abandoned for making permanent molds.

Therefore, among all the ceramic materials studied in this program, boron nitride produced the best results, but the material and processing costs were considered to be extremely high. Silicon nitride shows some promise if preheating will ameliorate the poor thermal shock resistance.

CONCLUSIONS

- 1 The experimental ferrous casting machine designed and built in this program appeared to be at least partly successful for both conventional and rheocasting process. But due to the complications in its construction and operation this design may not be practical for full scale production. Material still remains a major problem for ferrous casting. Instead of batch type operation as in this case, a continuous type process would be more economical.
- 2 The use of MHD valve for controlling metal flow in foundry applications seems highly questionable due to enormous power requirement, excessive heating of the metal, metal-air interface instability, etc. However, for a laboratory scale model its successful operation can be demonstrated.
- 3 For permanent mold application of graphite for ferrous casting, diffusion bonded carbide coating (by metallizing and/or diffusion annealing) is better than other coating techniques. The major problem of ceramic materials was their poor thermal shock resistance. Among the limited number of ceramic materials tested in this program, boron nitride appeared to have the best thermal shock resistance. Also its reaction with the ferrous alloys was very slow.

REFERENCES

- (1) E.C. Okress and D.M. Wroughton, Electromagnetic levitation of Solid and Molten Metals, J. Applied Phys., 23, p. 545 & 1413 (1952).
- (2) E. Fromm and H. Jehn, Brit. J. Appl. Phys., 16, p. 653 (1965).

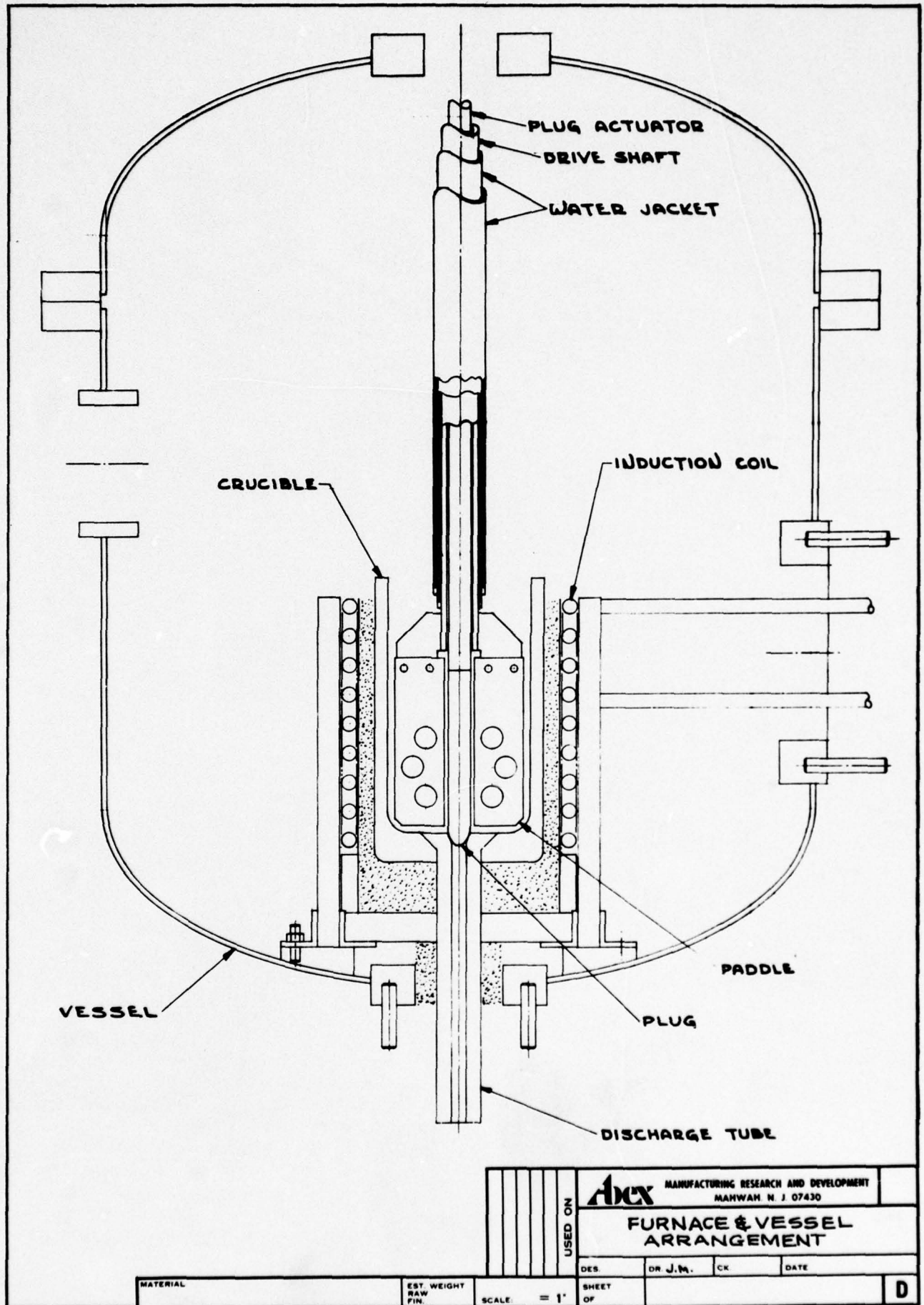
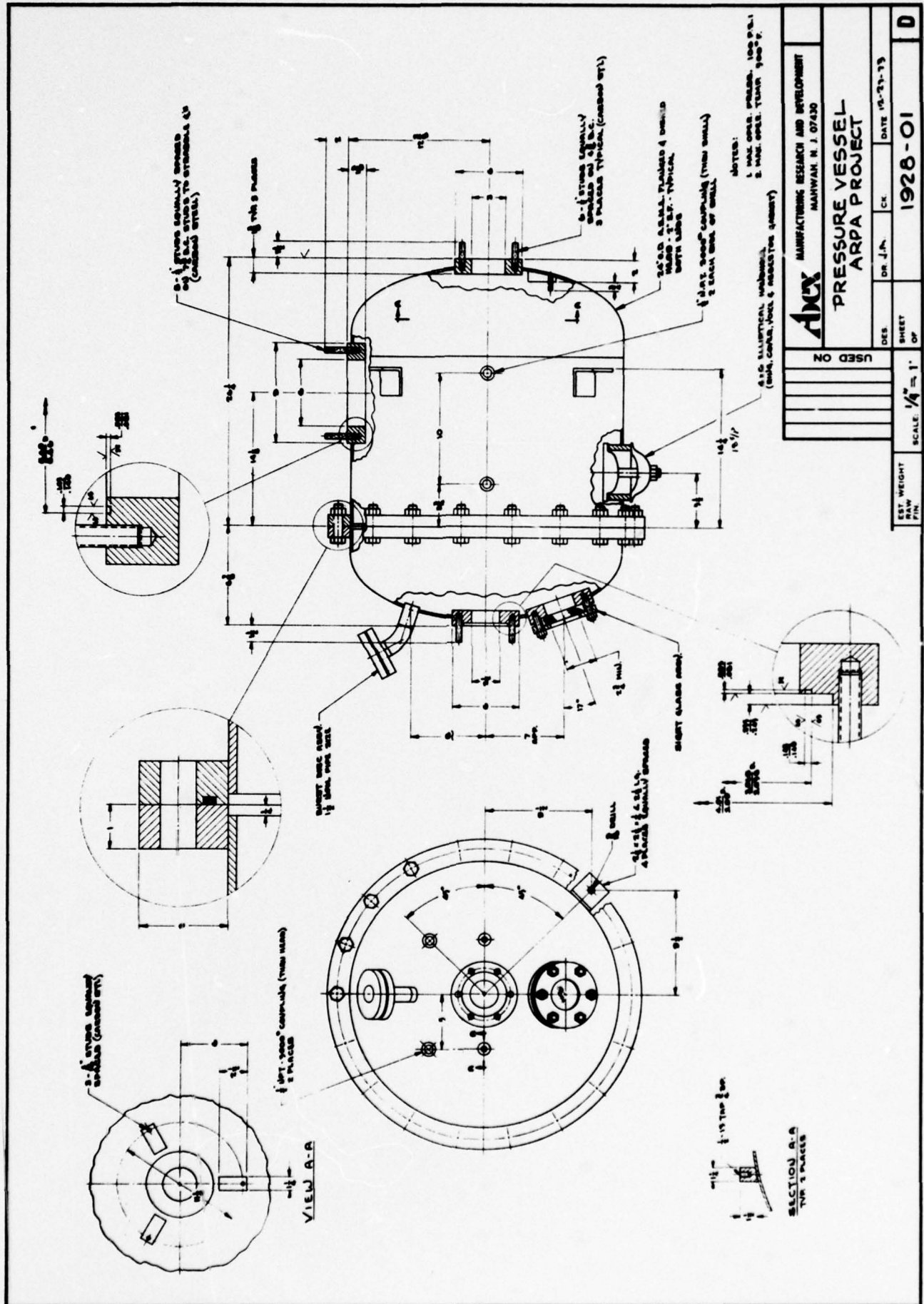
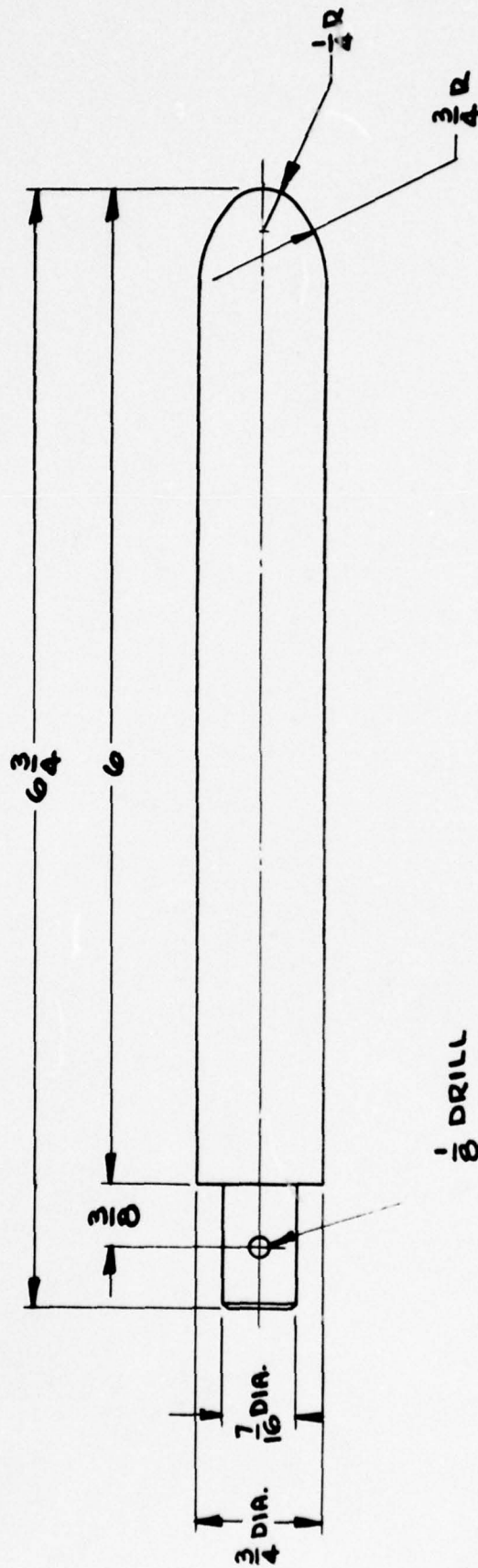


Figure 1. Furnace and Pressure Vessel Arrangement.

DES. DR. J.M. CK. DATE		USED ON	
		MATERIAL	
EST. WEIGHT RAW FIN.		SCALE = 1"	
SHEET OF		D	

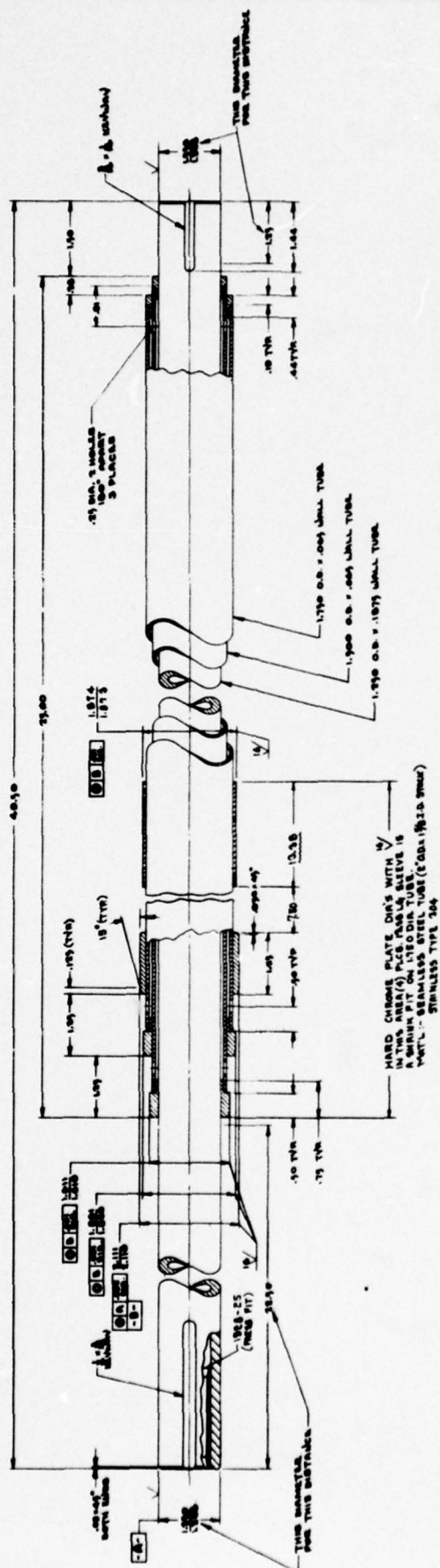
AMC MANUFACTURING RESEARCH AND DEVELOPMENT
 MANWAH N J 07430
**FURNACE & VESSEL
 ARRANGEMENT**





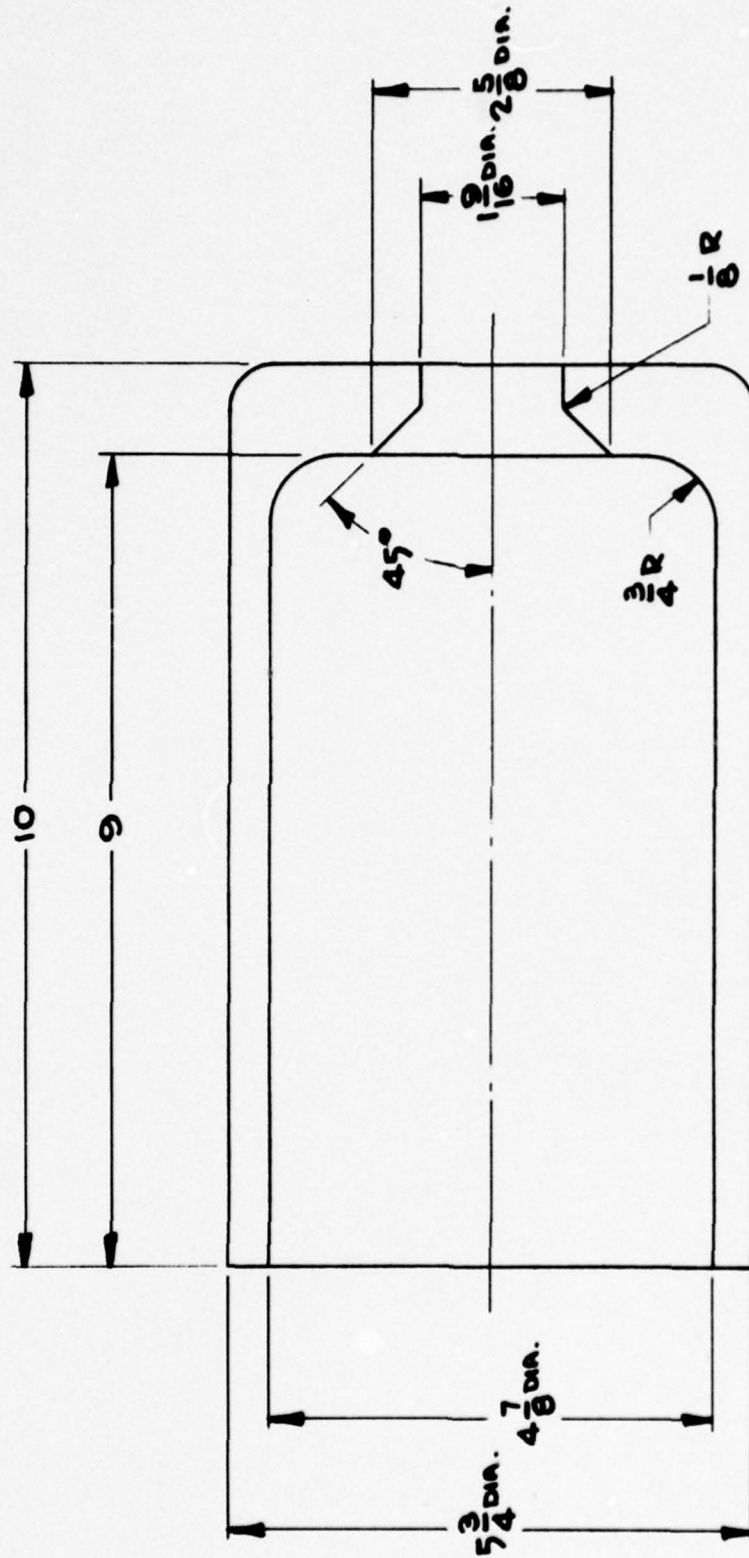
Aux		MANUFACTURING RESEARCH AND DEVELOPMENT	
		MANUFACTURING R. J. 07430	
NO. USED		PLUG	
ARPA PROJECT		DATE 10-21-73	
DES.	DR. J.A.	CL.	1928-04
SHEET	OF		
MATERIAL		EST. WEIGHT	SCALE 1" = 1'
		RAW	
		FIN.	

Figure 3. Stopper Rod.



Notes:
1. ALL JOINTS TO BE LEAK TIGHT @ 100 PSI WATER PRESSURE

Figure 4. Drive Shaft.



AMX MANUFACTURING RESEARCH AND DEVELOPMENT MANHATTAN N. J. 07430		CRUCIBLE ARPA PROJECT		DATE 12-28-73	B
DES.	DR. J.A.	CK.	1928-02		
USED ON			SCALE $\frac{1}{2}'' = 1''$		
EST. WEIGHT RAW FIN.					
MATERIAL					

Figure 5. Crucible.

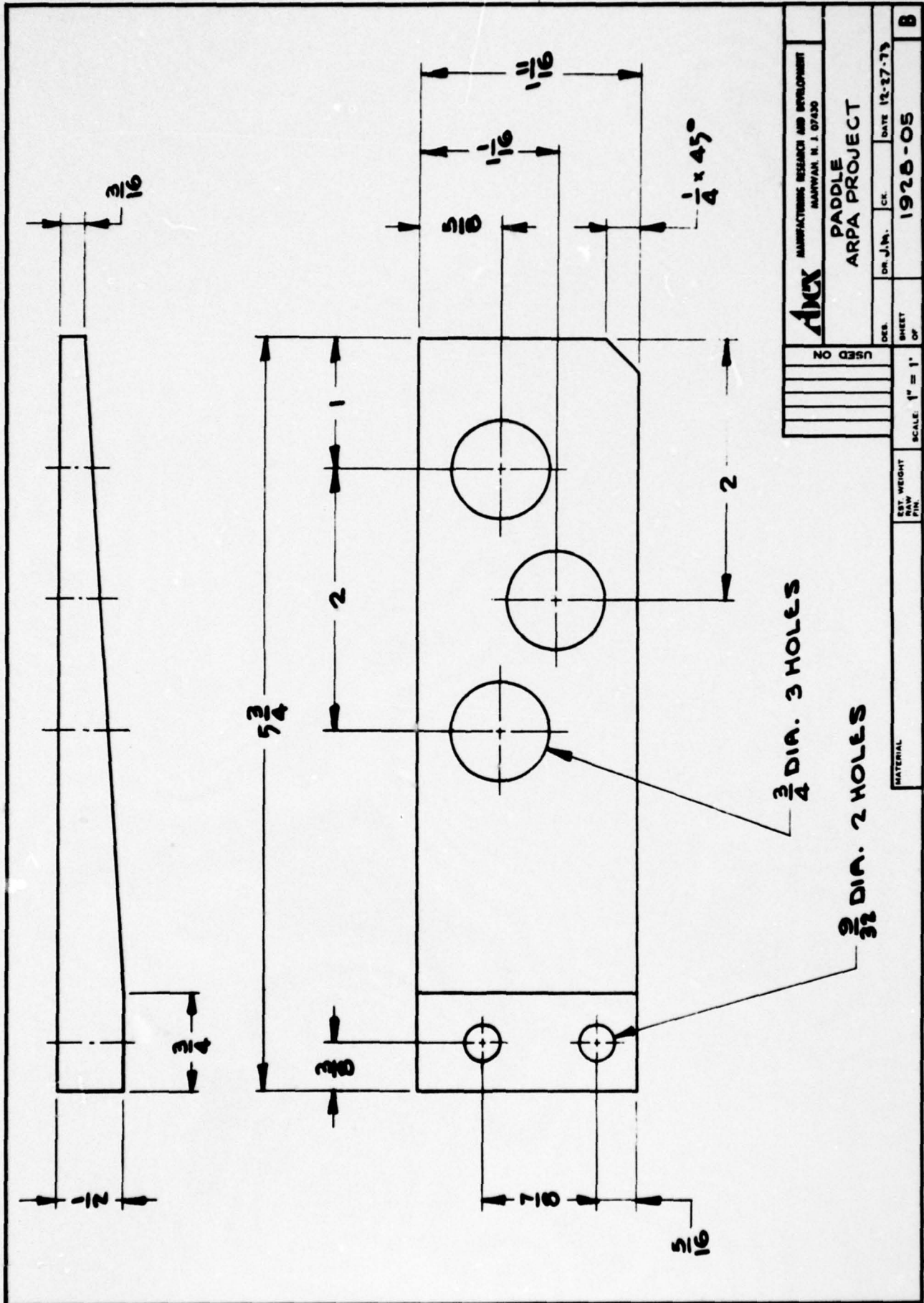
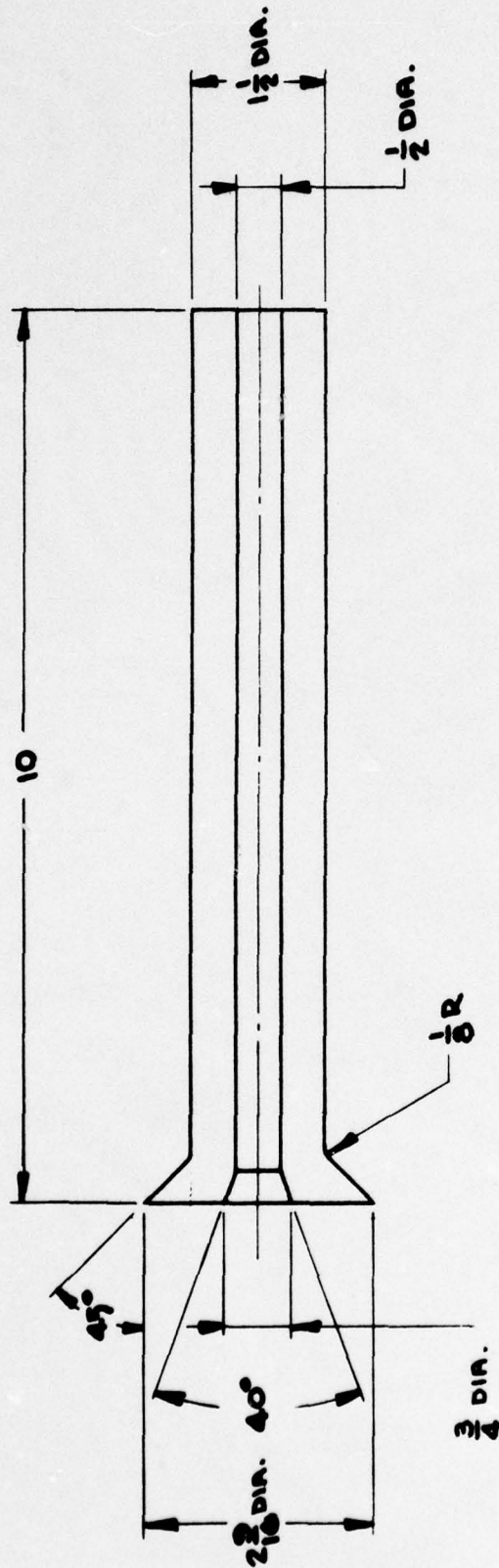


Figure 6. Stirring Paddles.



ACX MANUFACTURING RESEARCH AND DEVELOPMENT MANHATTAN N. J. 07430	
DISCHARGE TUBE ARPA PROJECT	
DES.	DR. J. M.
SHEET	CK
OF	DATE 12-26-73
SCALE: $\frac{1}{2}'' = 1'$	
MATERIAL	
EST. WEIGHT RAW FIN.	
1928-03	
B	

Figure 7. Discharge Tube.

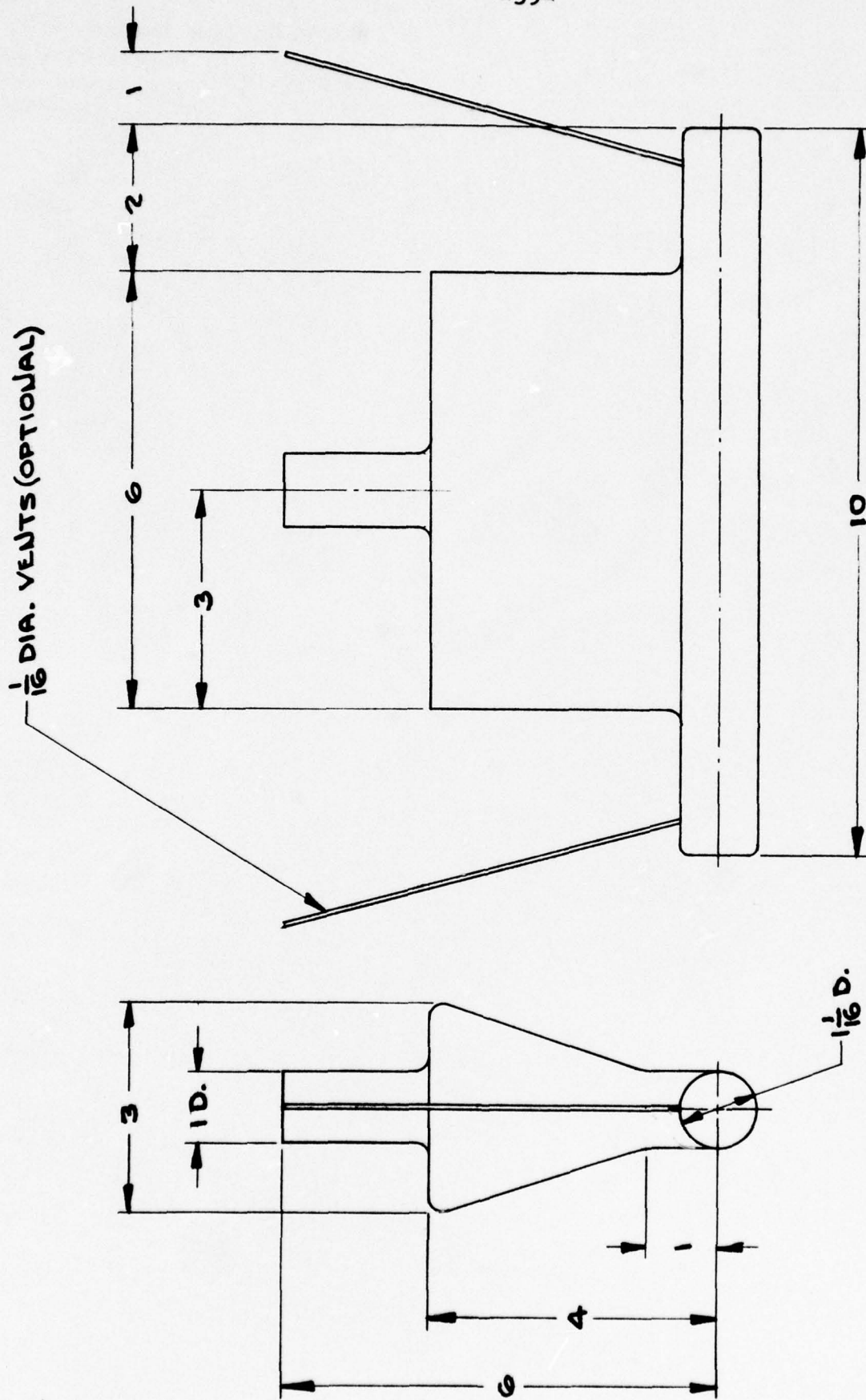


Figure 8. Abex Test Bar (D14)

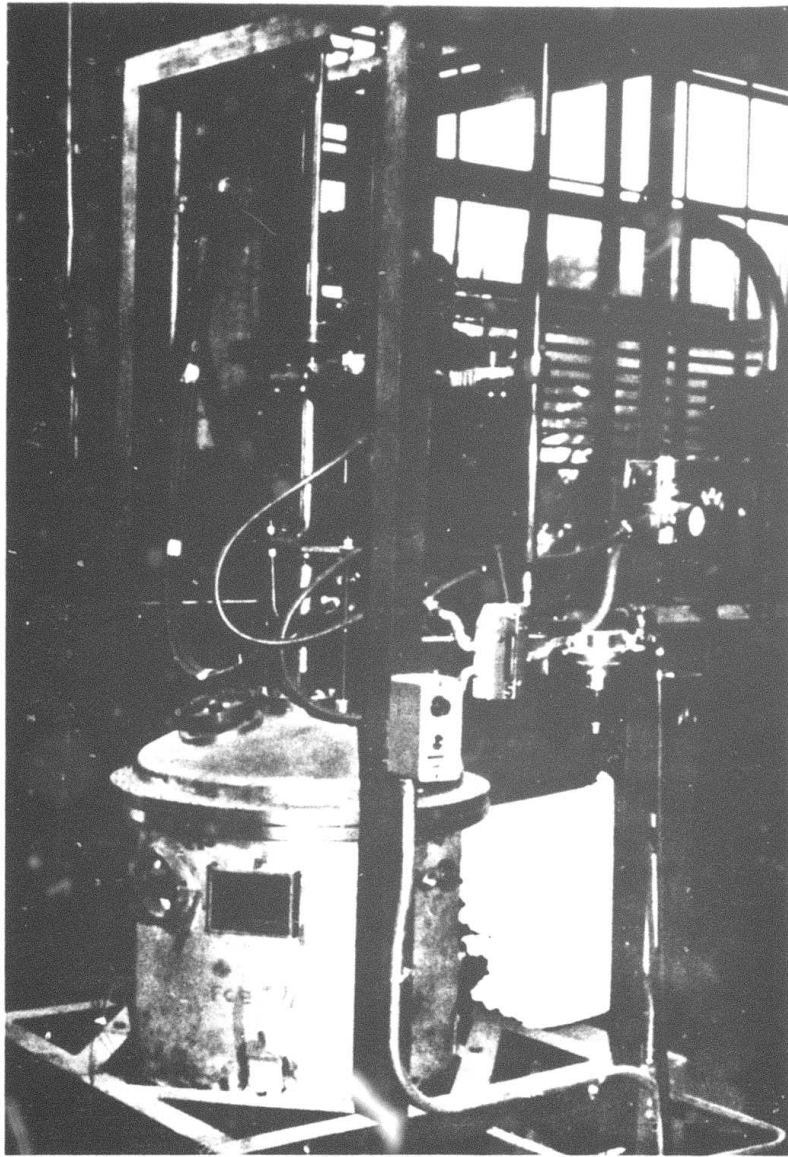


Figure 9(a). Experimental Melting and Casting Unit

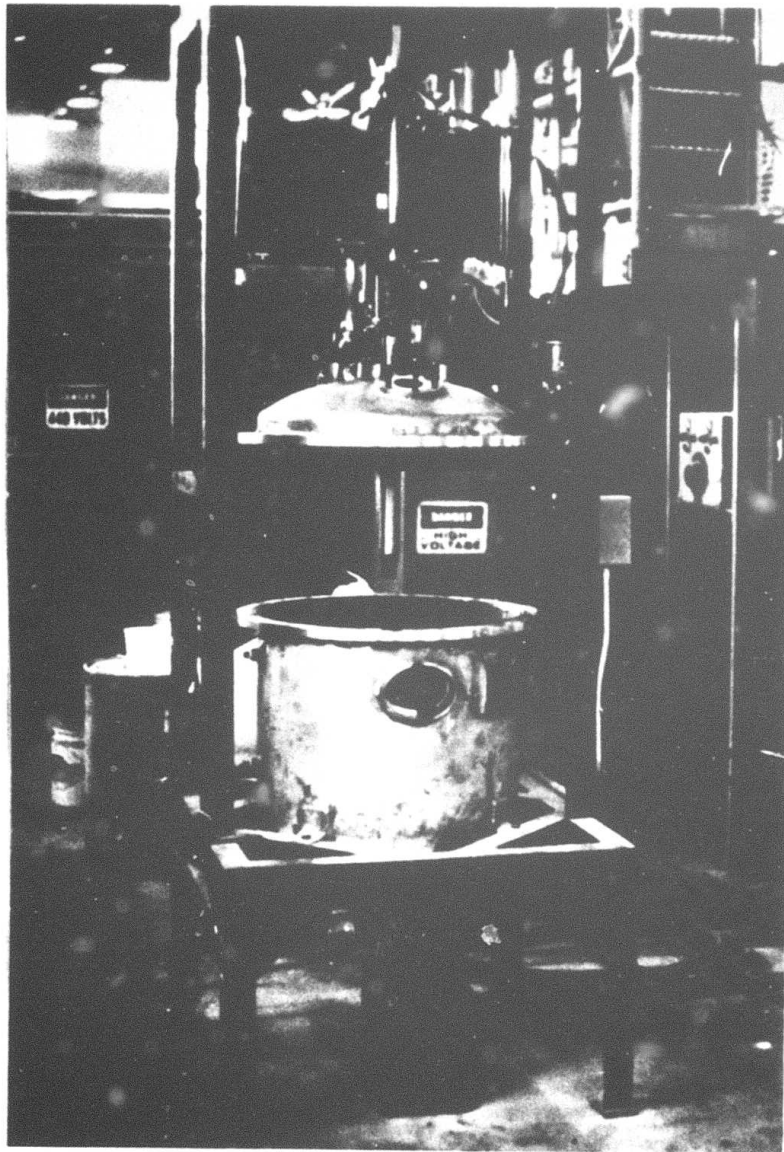


Figure 9(b) .Experimental Melting and Casting Unit

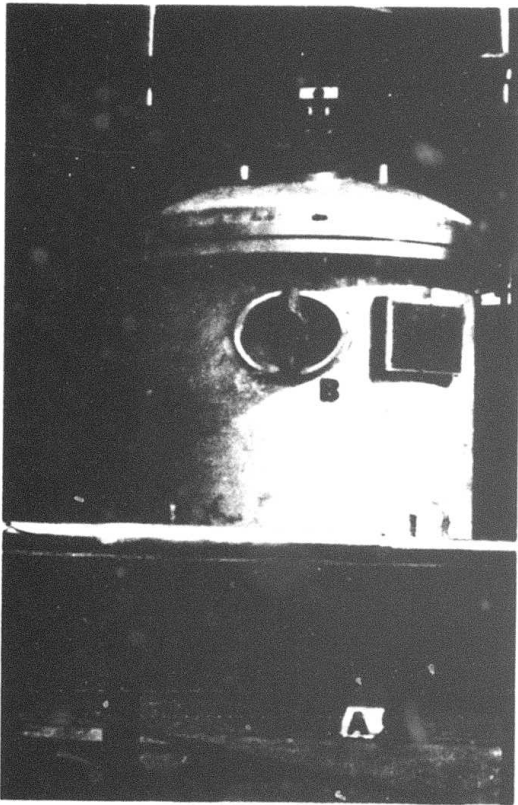


Figure 10.
Front View of Casting Unit
A Outlet
B Access Port

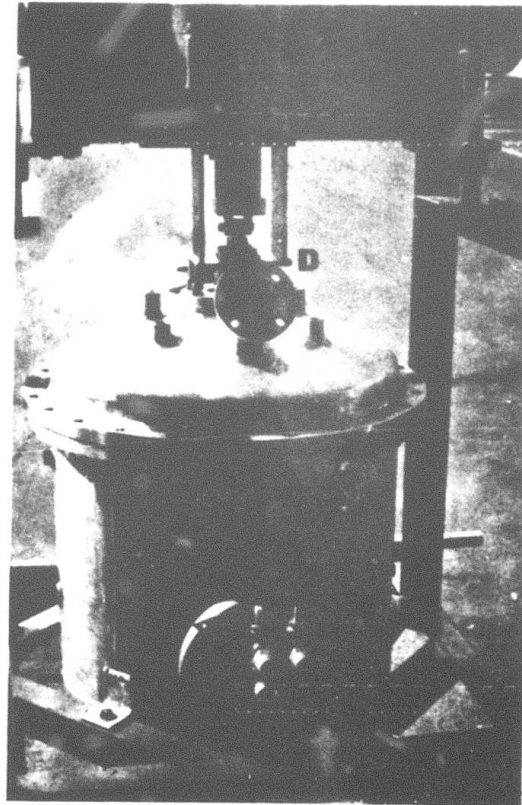


Figure 11.
Rear View of Casting Unit
C Induction Power Port
D Burst Disc Fixture

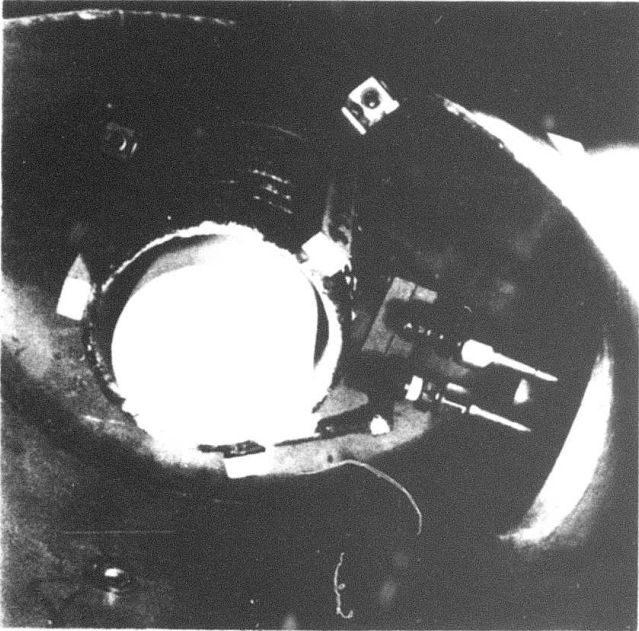


Figure 12.

Induction Coil With Crucible
in Place

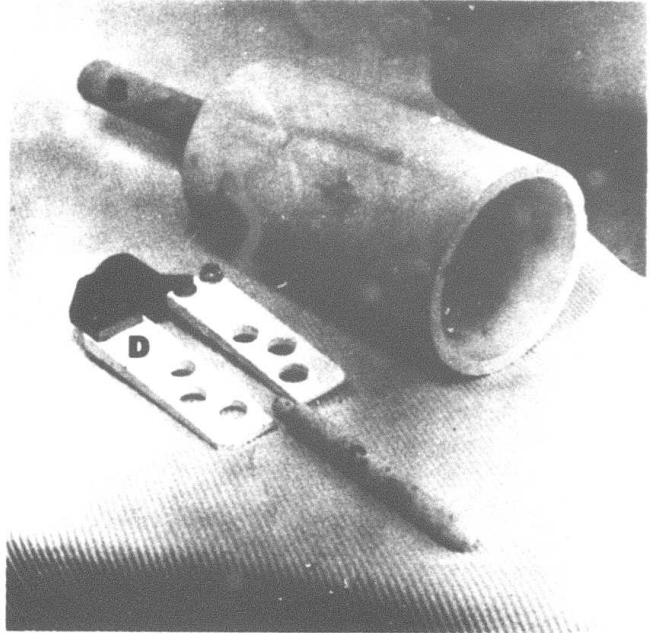


Figure 13.

Refractory Components of
Casting System

- A Alumina Crucible
- B Bottom Nozzle
- C Bottom Plug
- D Paddle Assembly

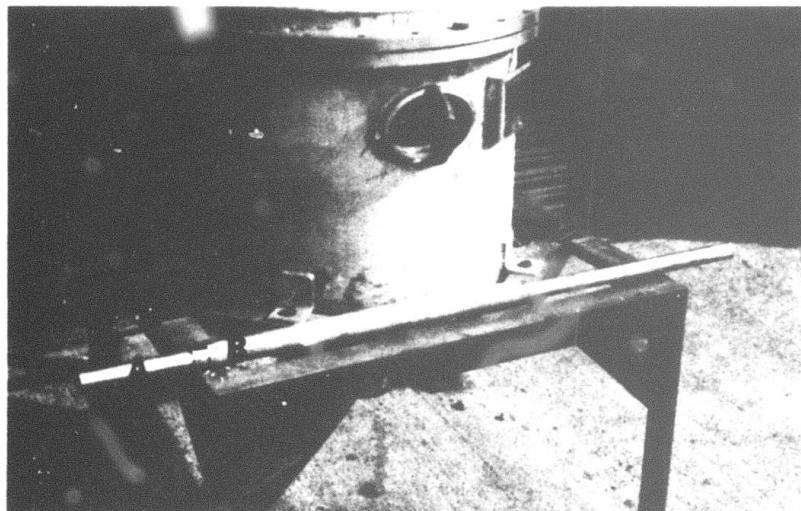


Figure 14.

Multiple-Function Shaft

- A Paddle Drive
 - B Cooling Jacket
- (Note: Plug Actuating Bar Not Shown)

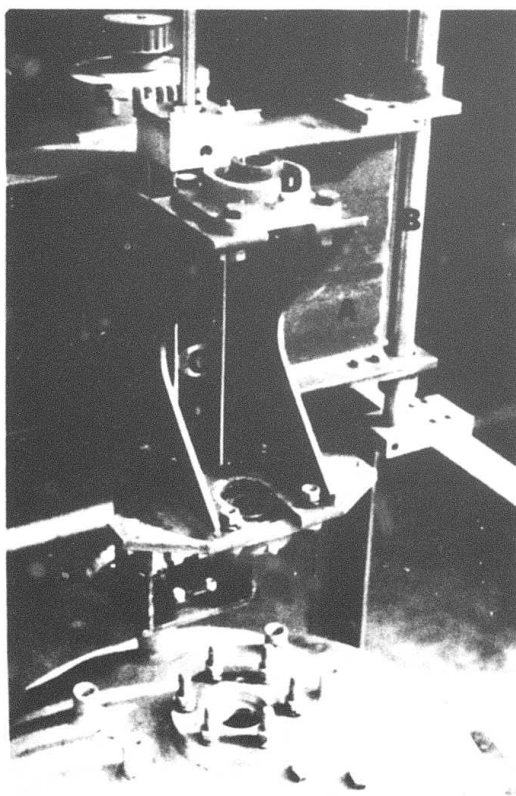


Figure 15.

Shaft Actuating Assembly

- A Support Beam
- B Guide Bars
- C Air Cylinder
- D Shaft Bearings
- E Paddle Drive Motor

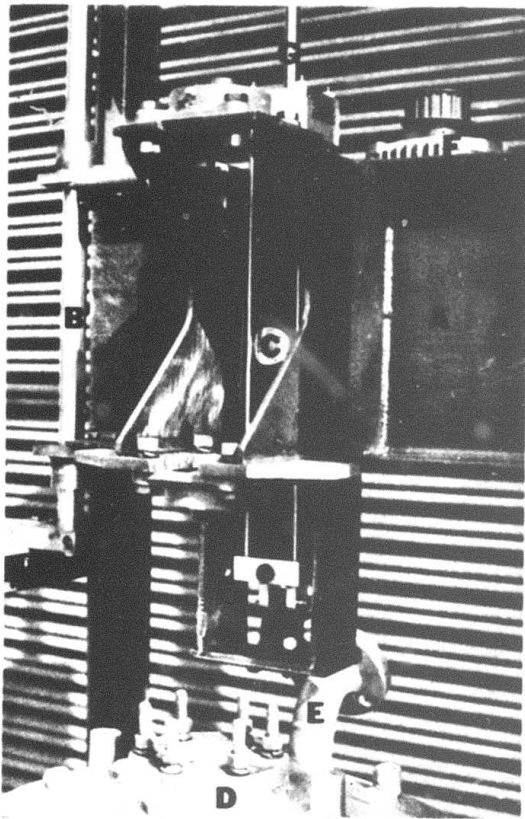


Figure 16.

Shaft Actuating Assembly

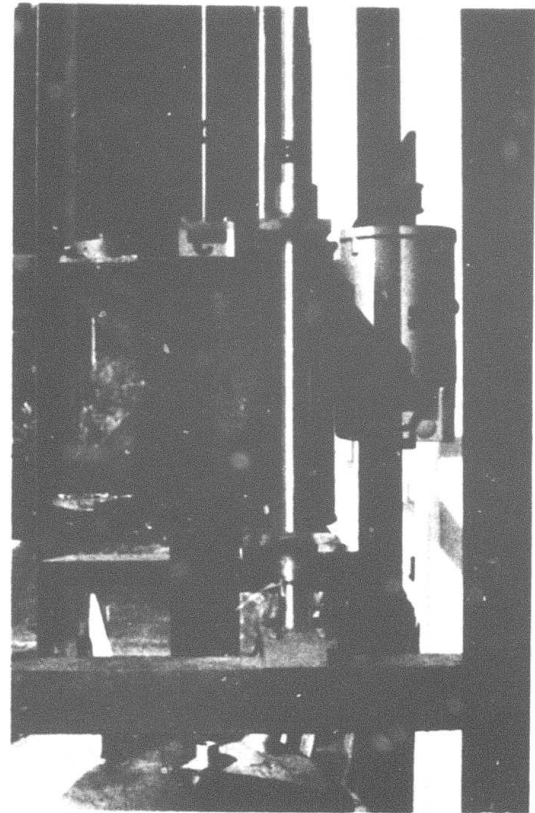
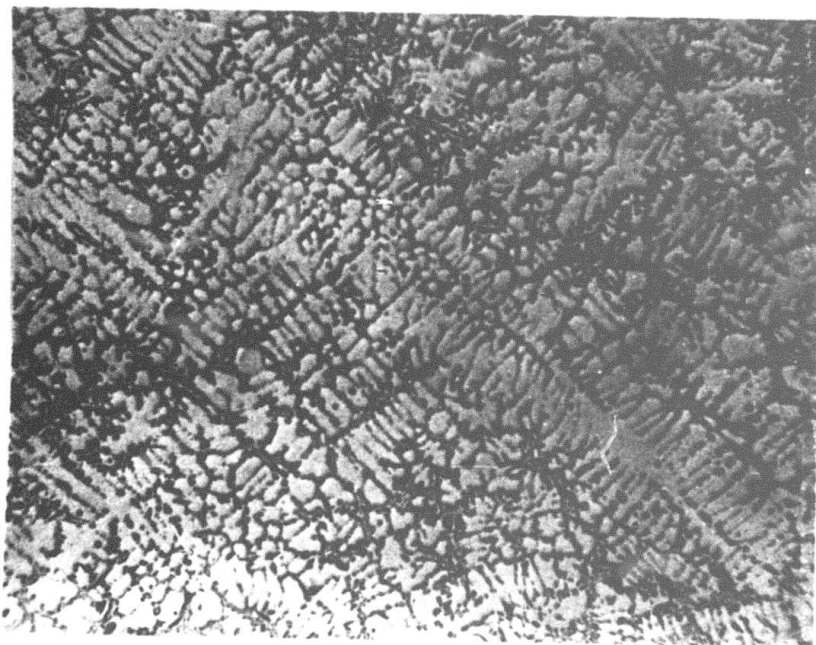


Figure 17.

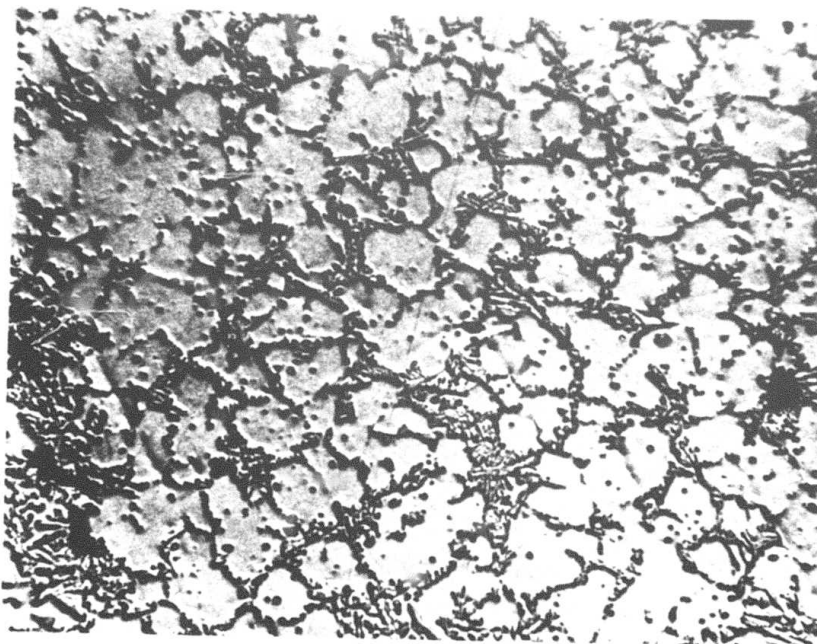
Shaft Actuating Assembly

- A Support Beam
- B Guide Bars
- C Air Cylinder
- D Casting Chamber Access
- E Burst Disc Fixture
- F Paddle Drive Motor
- G Fixed Air Cylinder Shaft



AW116701 50X

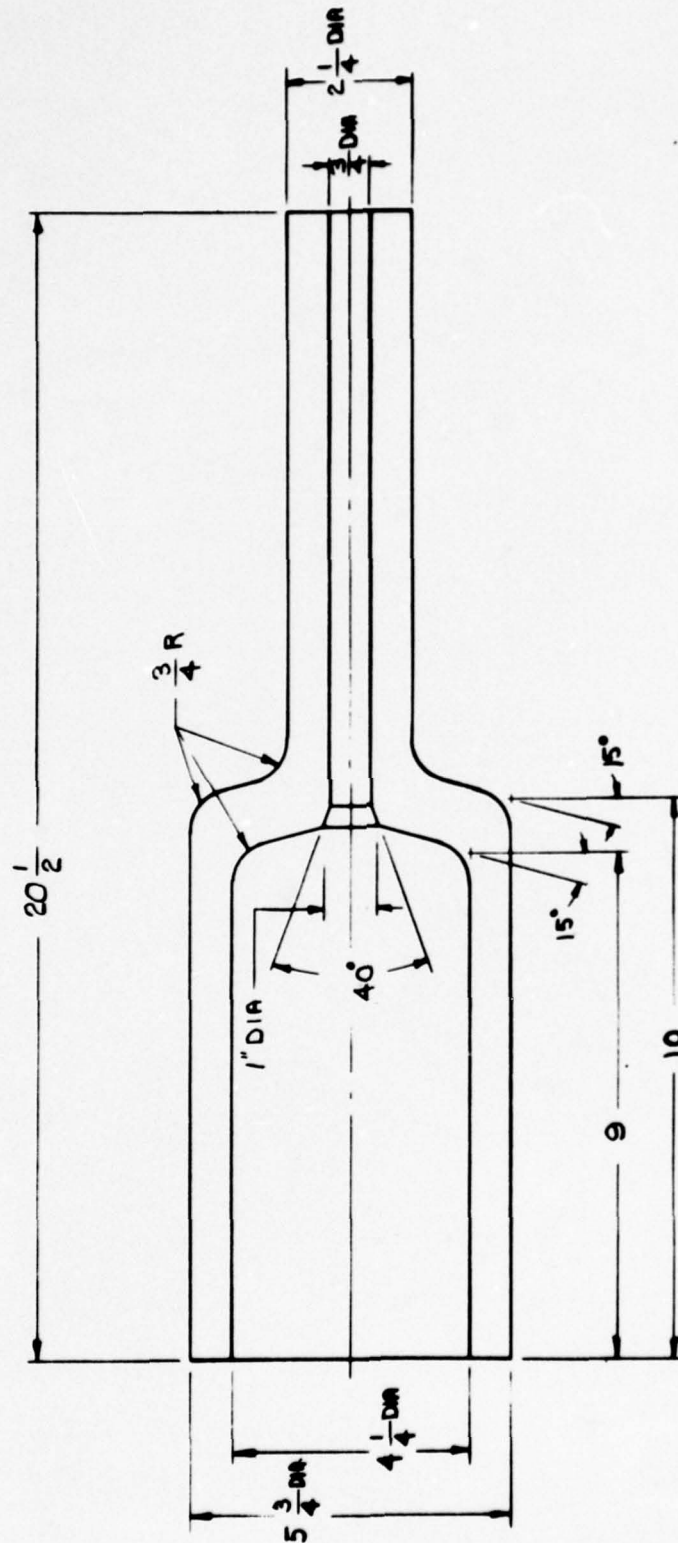
(a) Conventionally Cast



AW116601 50X

(b) Rheocast at About 0.5 Solid Fraction

Figure 18. Micrographs of Conventionally Cast and Rheocast 356 Alumina Base Alloy (Al-7% Si).



		CRUCIBLE - FURNACE ARPA PROJECT		DES. DR. SCHMIDT DATE 3-31-75
SHEET 1 OF 1		SCALE 1/2" = 1"		B
MATERIAL		EST. WEIGHT RAW FIN.		1928-17
ALL UNFINISHED SURFACES TO BE 100%		TOLERANCE ON FINISHED SURFACES ANGLES ± 1/2°		1928-17

Figure 19. Modified Crucible.

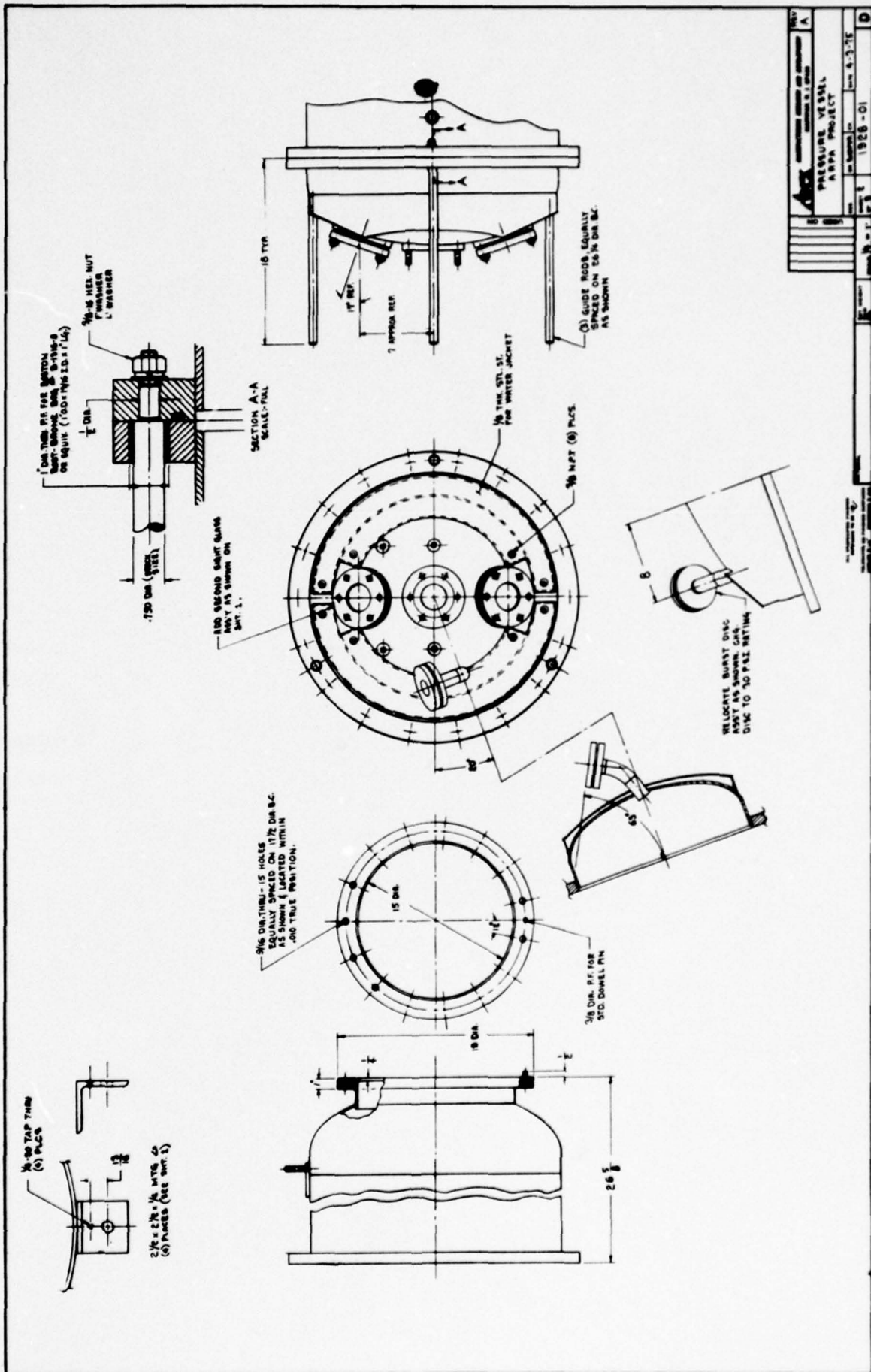


Figure 20. Modified Pressure Vessel.

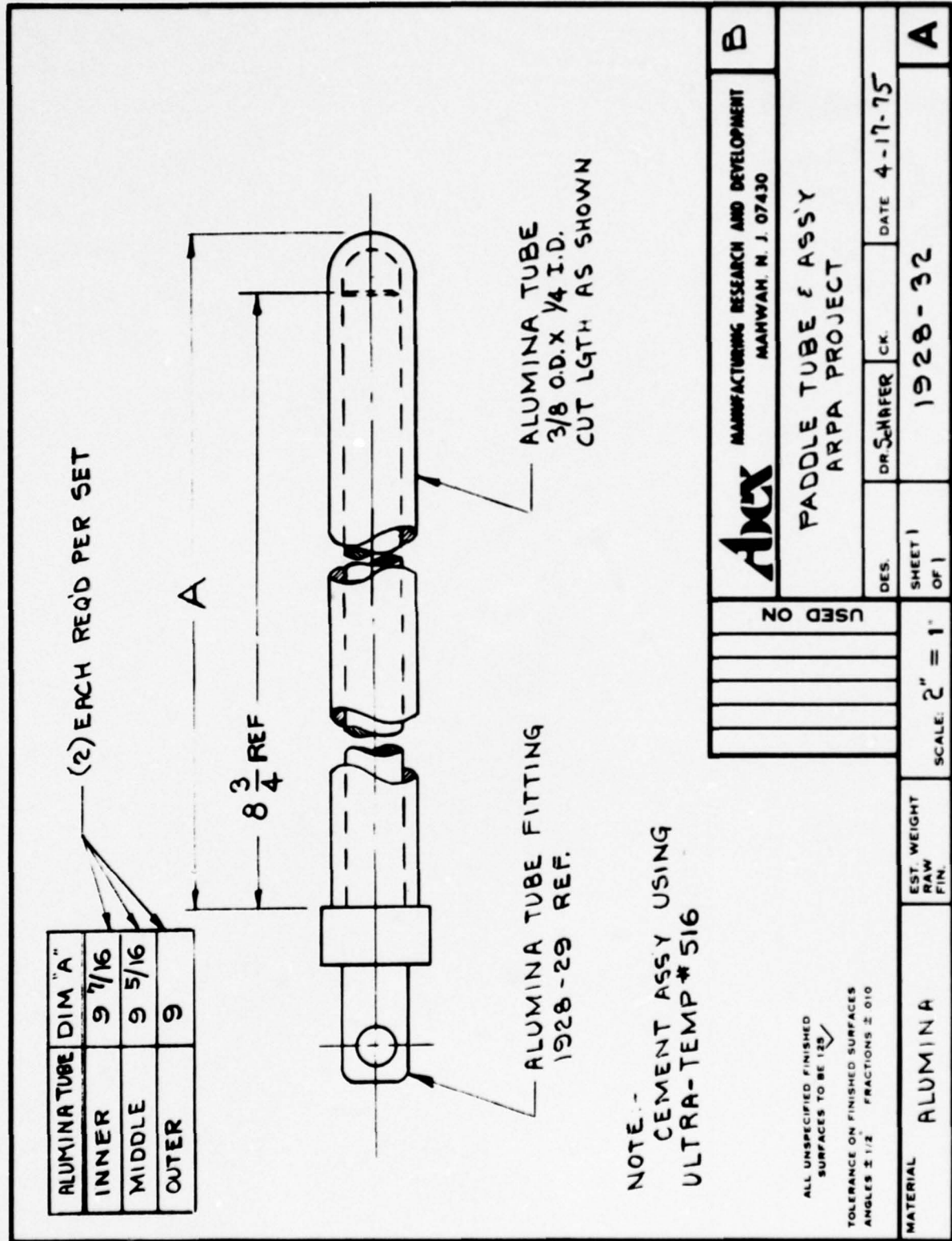
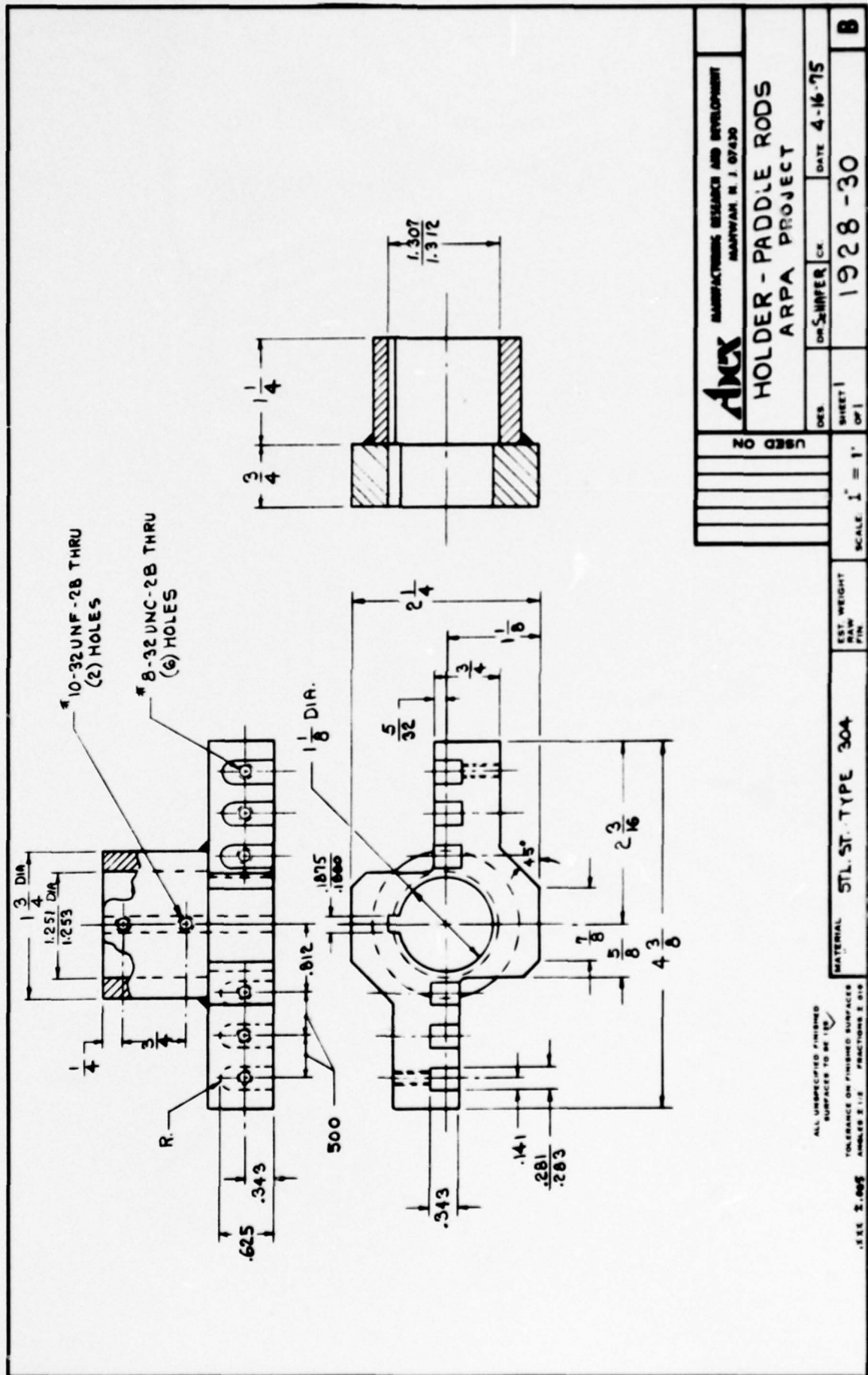
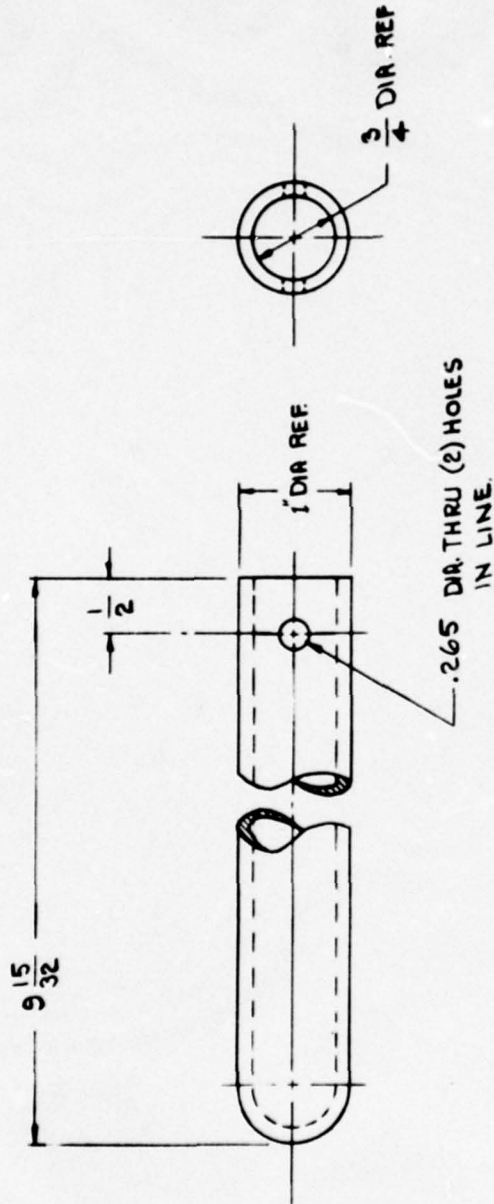


Figure 21. Stirring Rod and Assembly.





NOTE:-
STANDARD ALUMINA TUBE (COE)
EXCEPT AS SHOWN


 MANUFACTURING RESEARCH AND DEVELOPMENT MAHWAH, N. J. 07430		DES. DR. SCHAFER CK. DATE 4-11-75	
USED ON		PLUG - CRUCIBLE ARPA PROJECT	
MATERIAL ALUMINA		SHEET 1 OF 1	
EST. WEIGHT RAW FIN		SCALE 1" = 1"	
ALL UNSPECIFIED FINISHED SURFACES TO BE 125		1928-24	
TOLERANCE ON FINISHED SURFACES ANGLES ± 1/2 FRACTIONS ± .010		B	

Figure 23. Modified Stopper Rod.

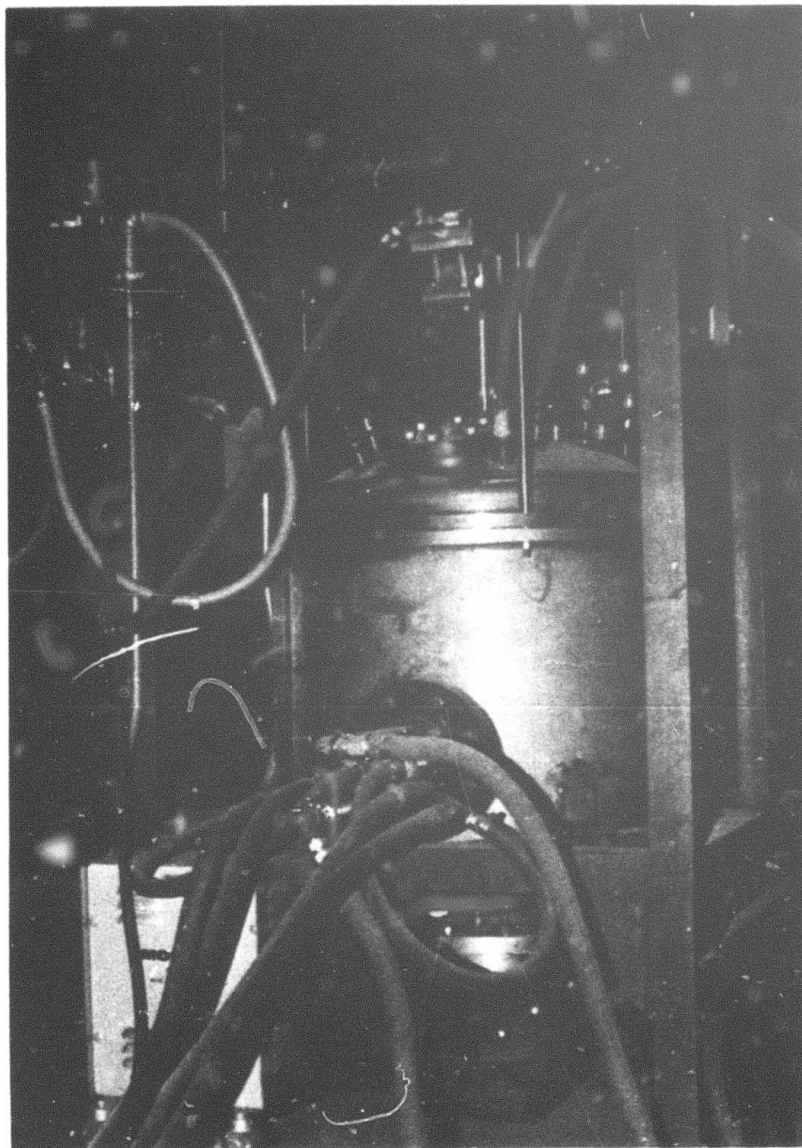


Figure 24(a). Modified Furnace and Pressure Chamber Assembly.

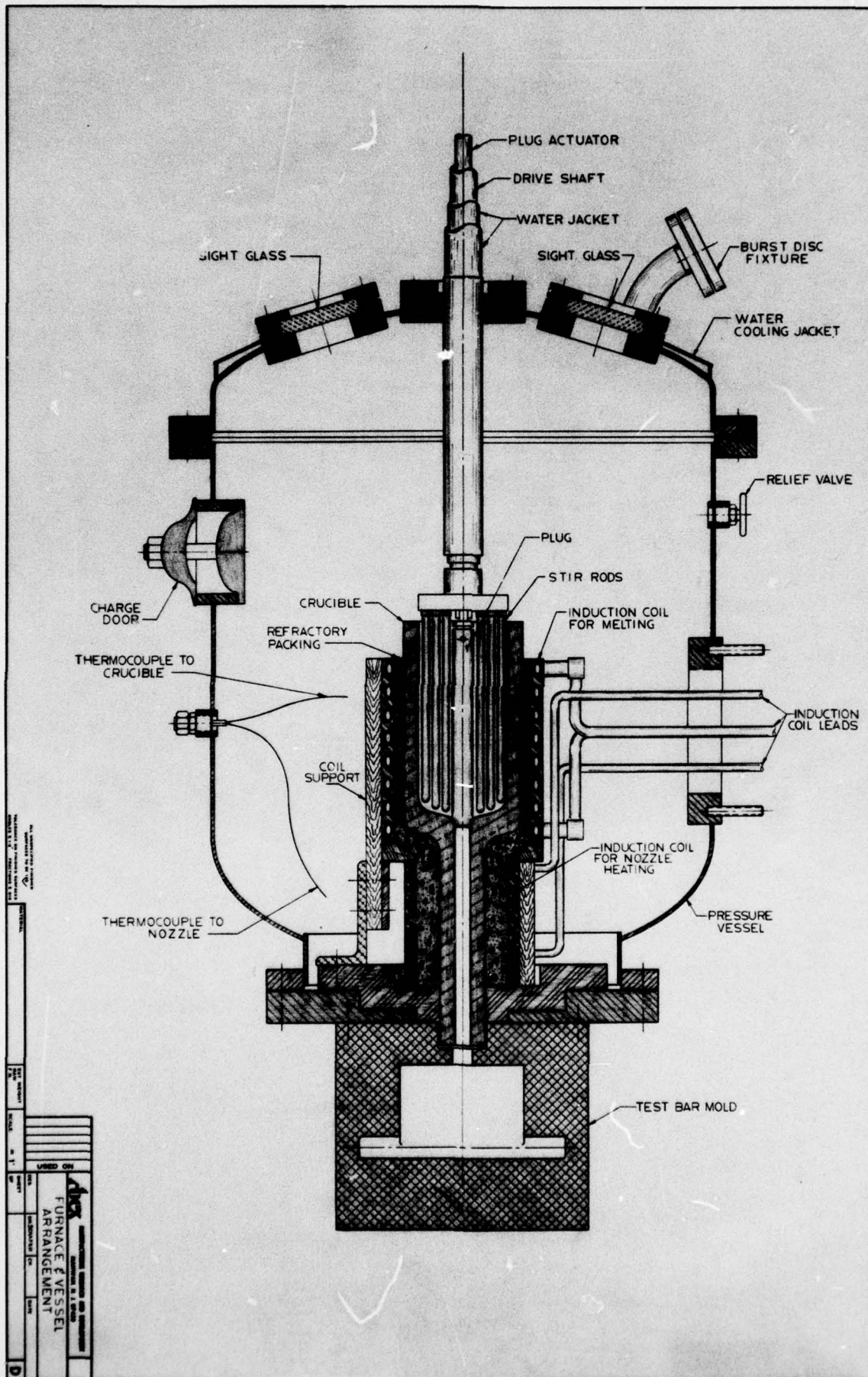


Figure 24(b). Modified Furnace and Pressure Chamber Assembly.

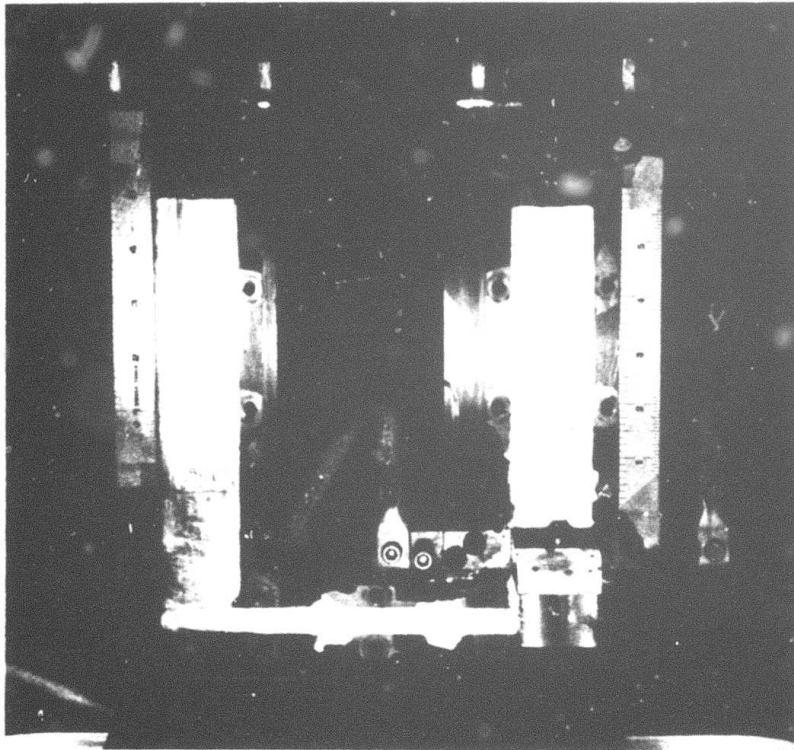


Figure 25. MHD Conduction Pump.

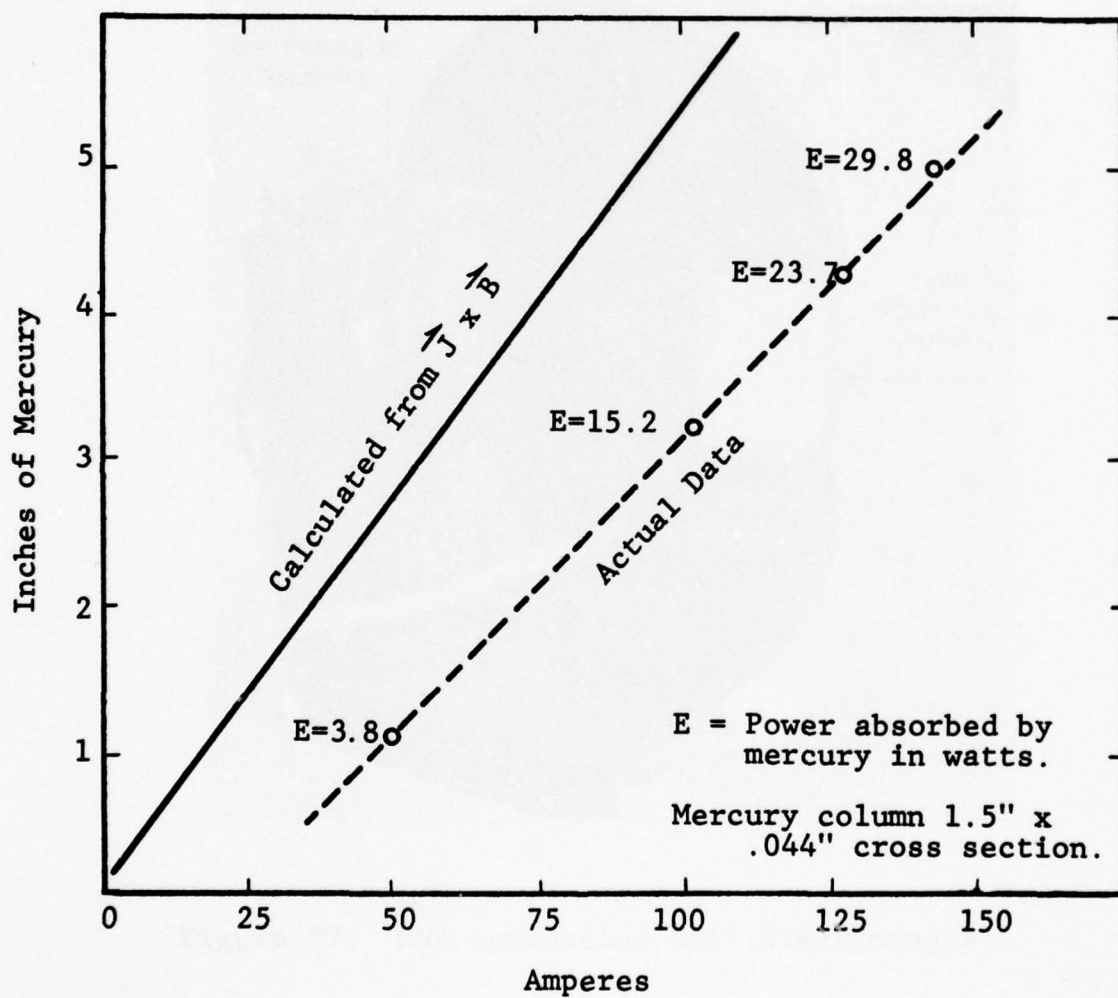


Figure 26. Theoretical and Actual Performance of Conduction Pump.

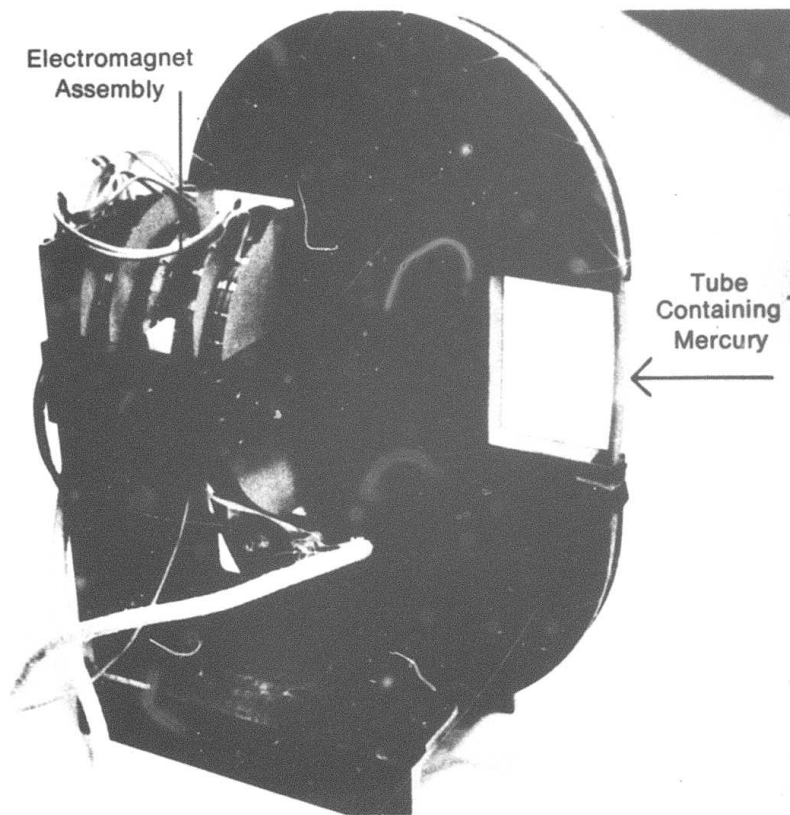


Figure 27. MHD Conduction Cell Electromagnet.

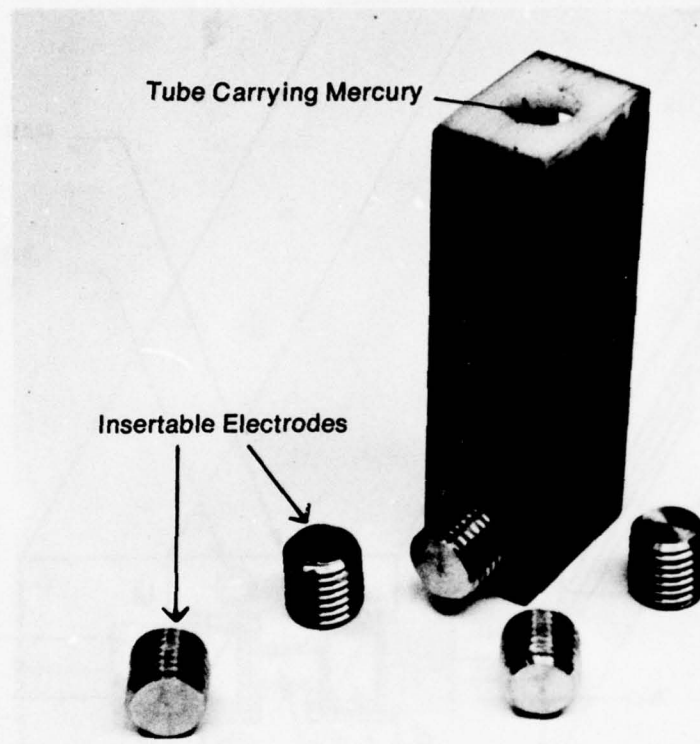


Figure 28. Multiple Electrode Assembly.

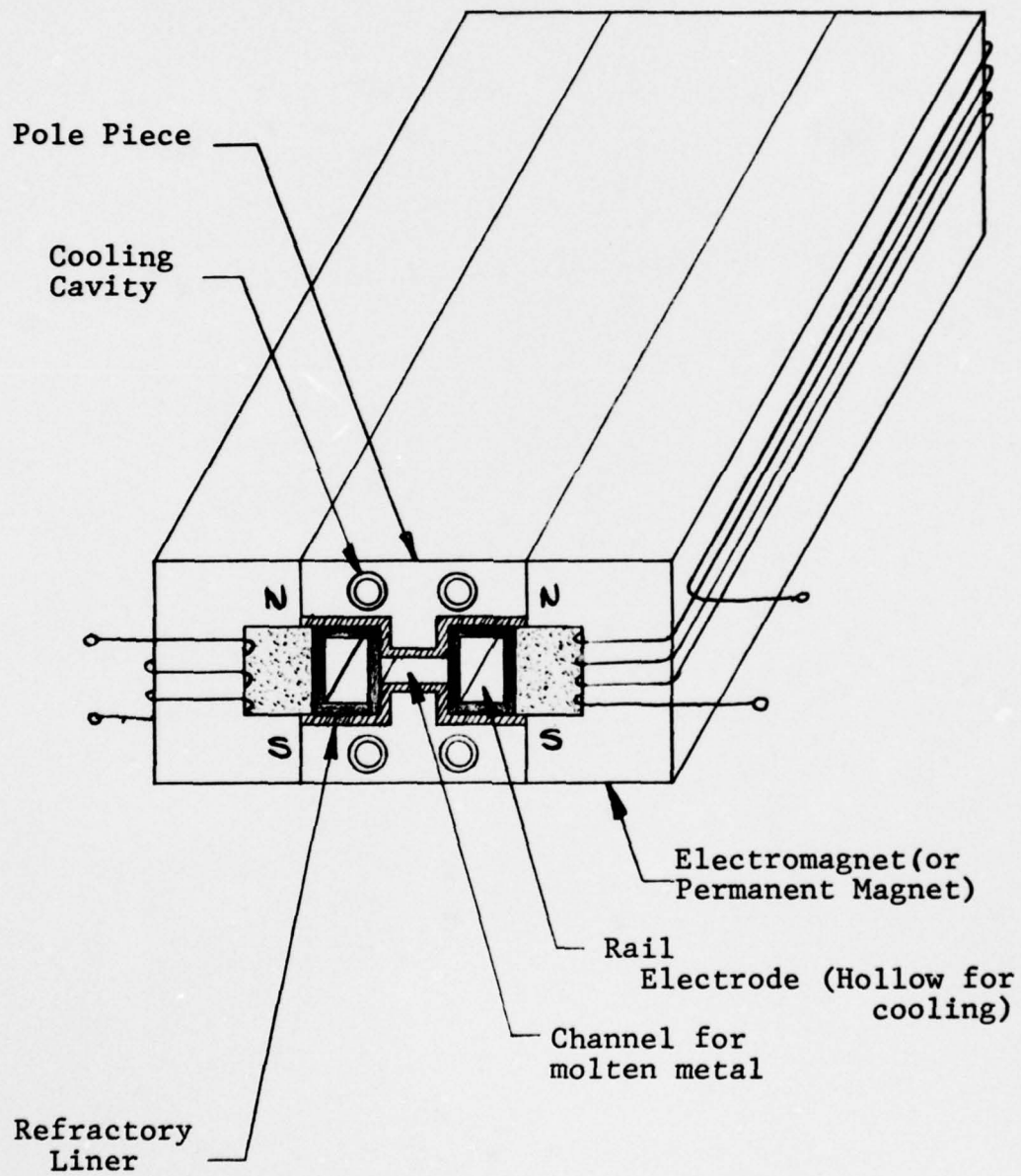


Figure 29. Rail Propulsion Conduit and Valve

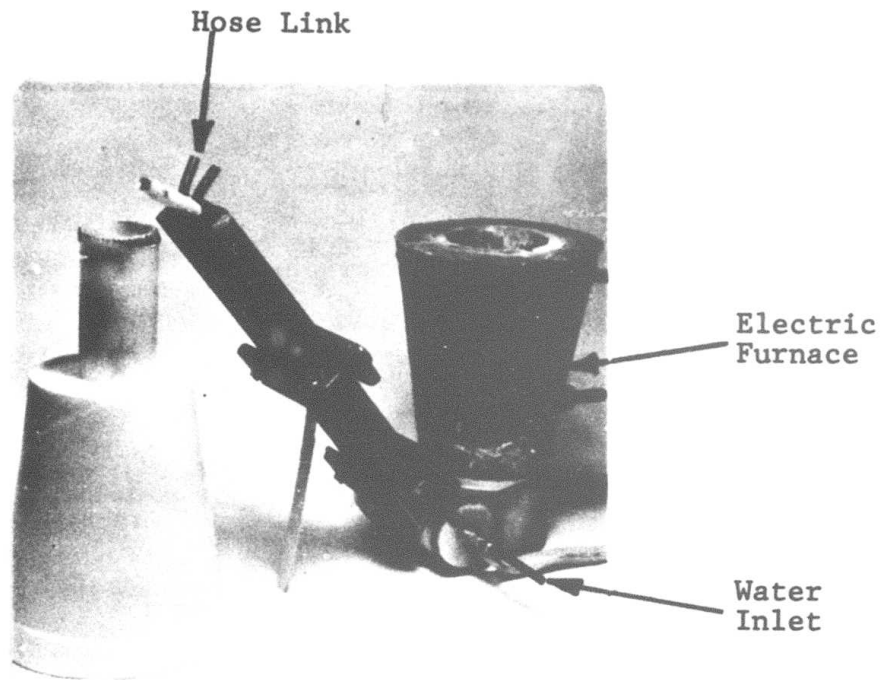


Figure 30. Rail Propulsion Conduit
Adjusted to Pour Up

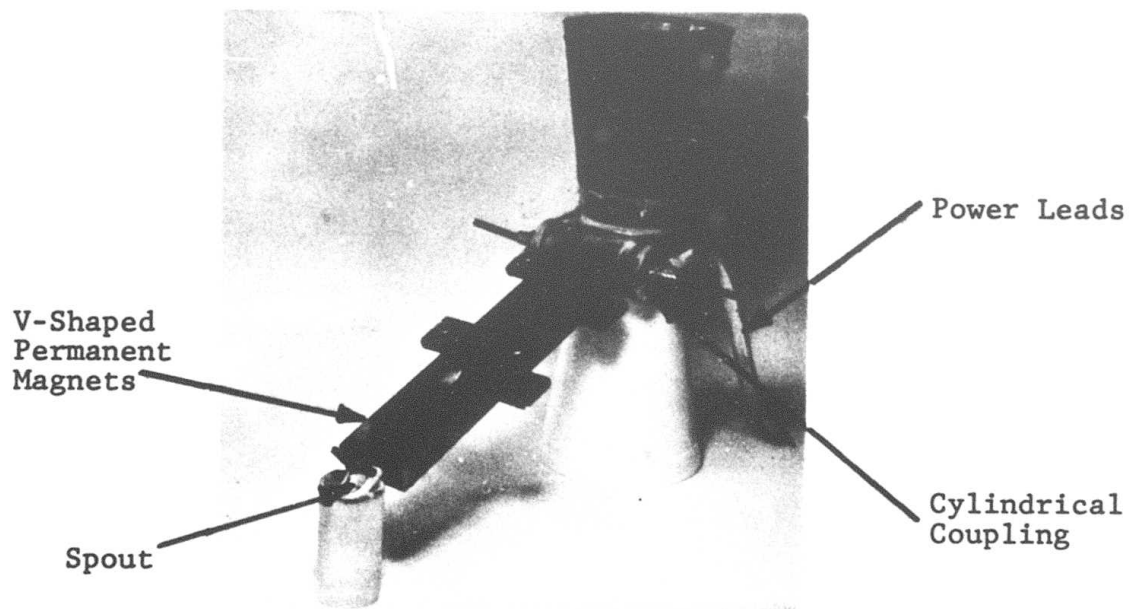


Figure 31. Conduit Used as Valve
for Gravity Pouring.



Figure 32, Conical Induction Coil for Levitation.

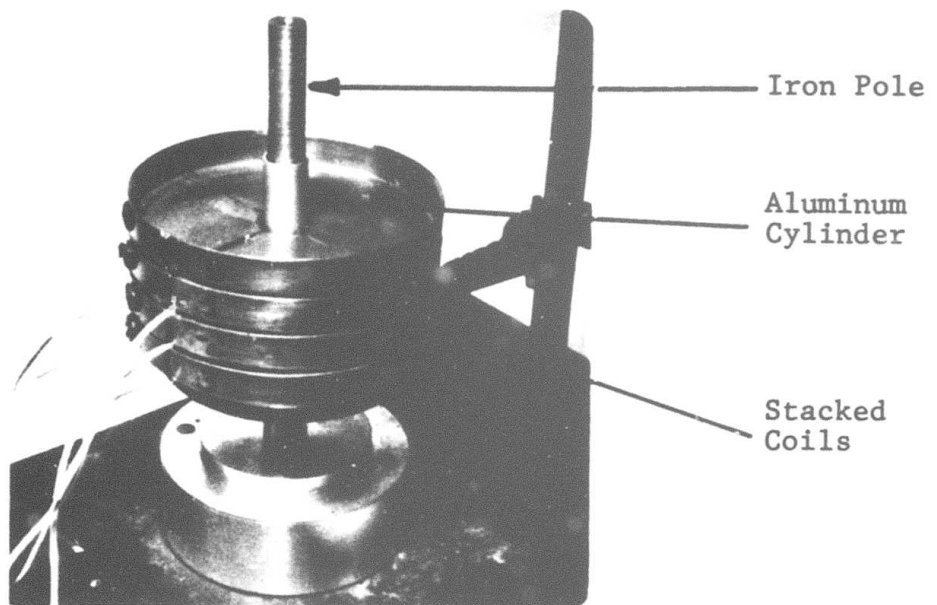


Figure 33. Polyphase Levitation Pump With Mu-Metal Flux Concentrators

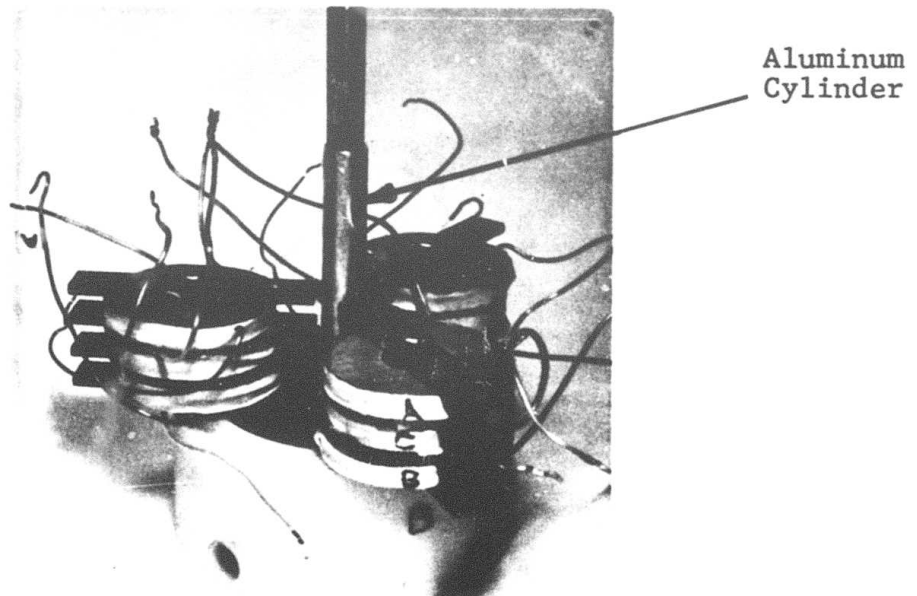


Figure 34. Three-pole, 3-Phase Levitation for Lift and Rotation

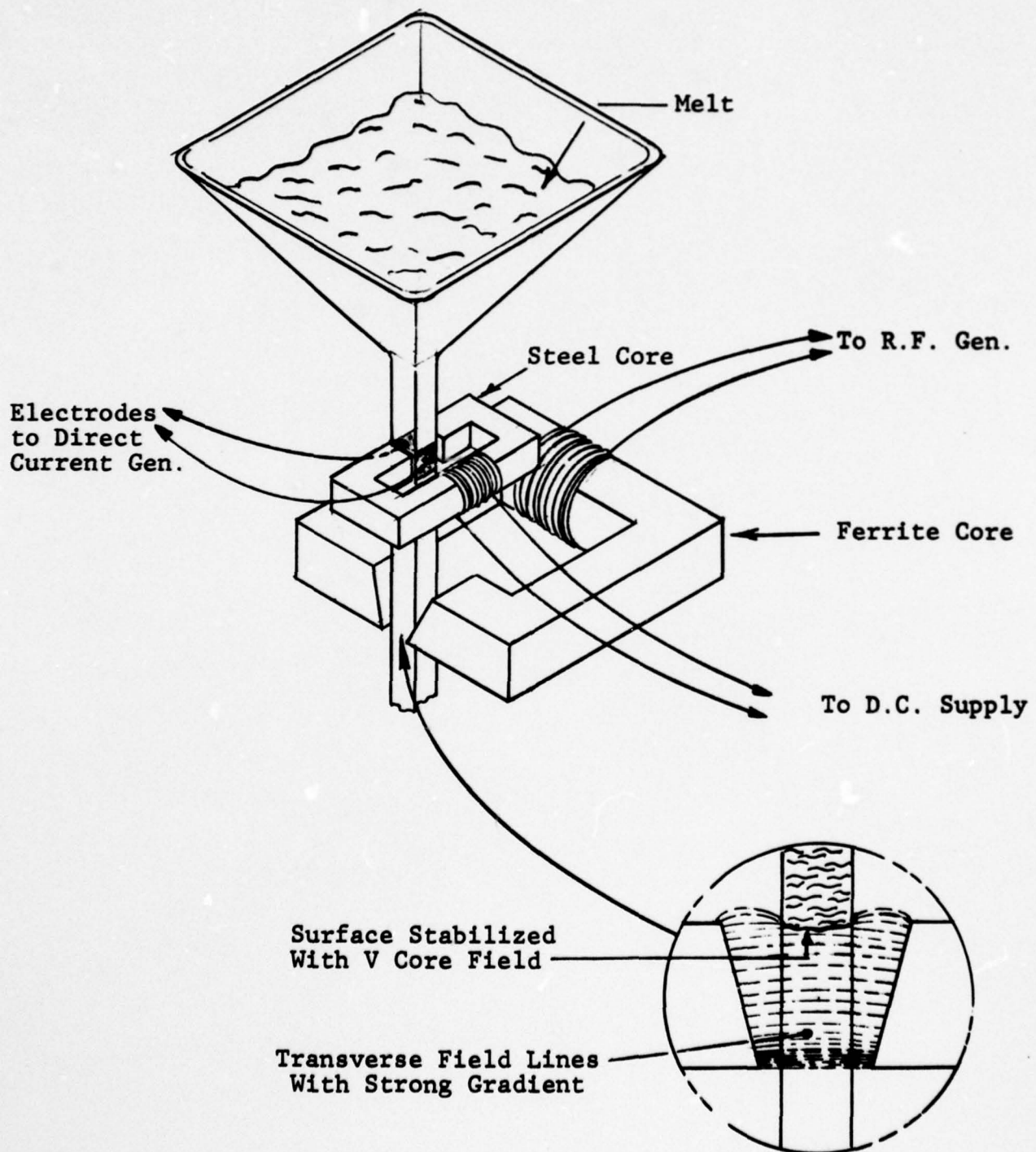


Figure 35. MHD Conduction Cell With Lower Surface Stabilized by A.C. Field

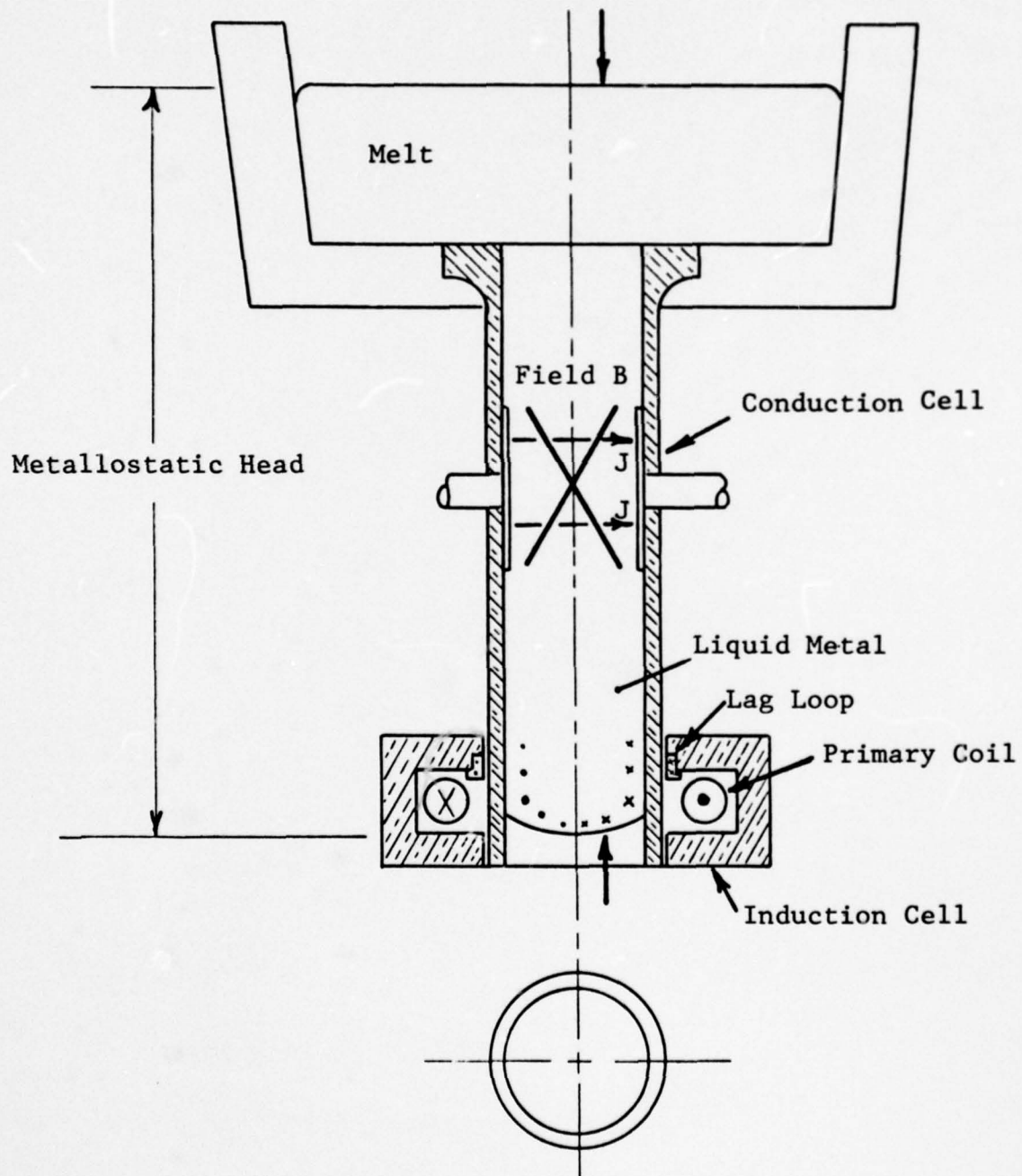
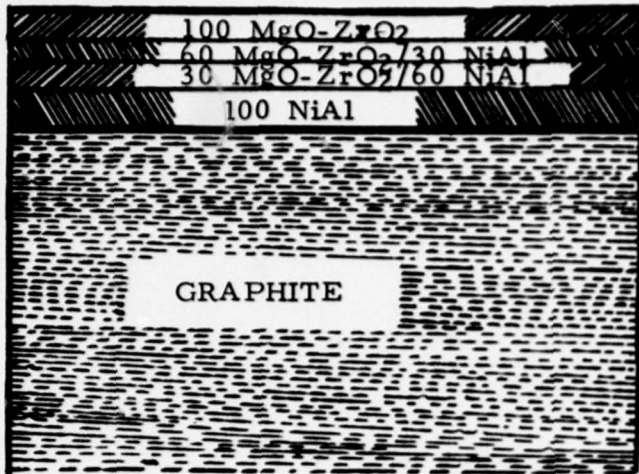
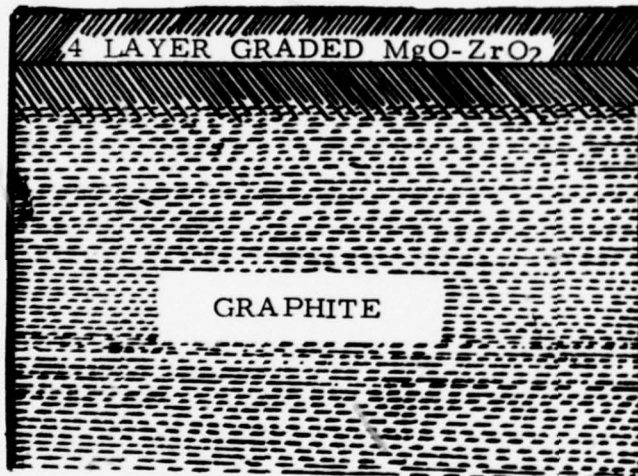


Figure 36. MHD Induction Conduction Cell With Lag Loop.

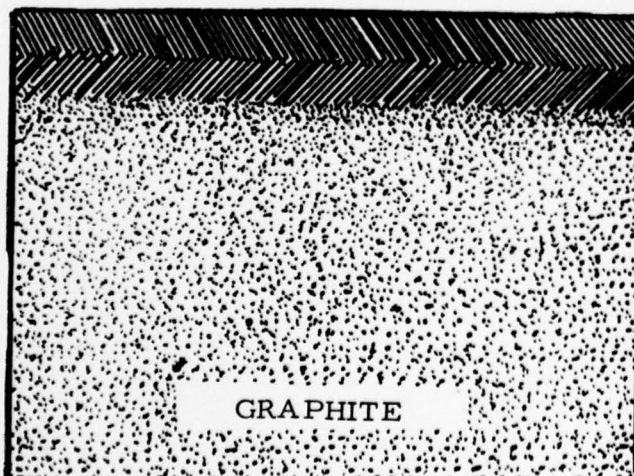


(a) Plasma Sprayed Four Layer Graded MgO-ZrO₂ Coating On Graphite Surface.



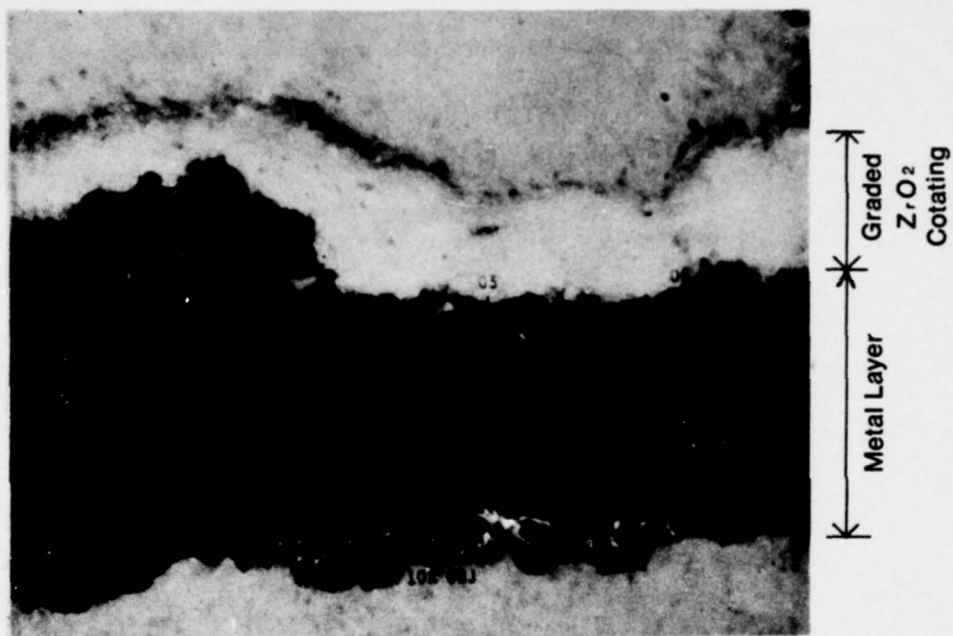
Diffusion Bonded Carbide Coating.

(b) Plasma Sprayed Four Layer Graded MgO-ZrO₂ Coating on Diffusion Bonded Carbide Layer of Graphite.



(c) Diffusion Bonded Oxide-Carbide Coatings on Graphite.

Figure 37. Multiple Layer Graphite Coatings.



100X

Figure 38. Micrograph (Taken Using Polarized Light) Showing Layer of Metal Underneath the Coating.

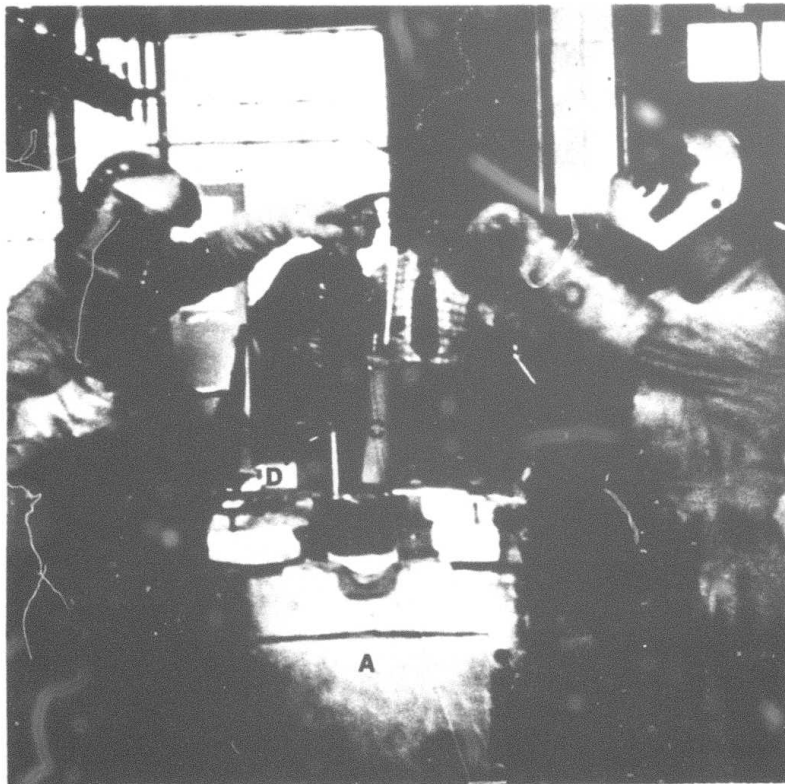


Figure 39. Dip Test Experiment.